Politecnico di Torino

Master's Degree in Mechatronic Engineering

A.a. 2020/2021

Development of a tunable dynamic-braking control model

Thesis Supervisor

Prof. Andrea Mura

Candidate

Guglielmo Dutto

Abstract

As technology progresses, ever more reliable and maintenance-free systems must be developed in order to keep up with the constantly growing demand in automation. A field where this necessity becomes all the more noticeable is the world of power electronics. Any newly designed machine has to be thoroughly tested through all of its possible states before it is deemed ready for deployment. This process is usually very expensive, both in terms of time and in terms of resources, considering the wear on components and the long and tedious procedures to be followed.

This work has the aim of finding a possible solution to this situation through the development of a tunable dynamic braking strategy, which would then be implemented as part of a test bench, exploiting a resistive element for electrical power dissipation and therefore braking torque generation. In particular, the precise control of MOSFETs through a pulse-width modulated signal output by a microcontroller board will allow for fine adjustments of the braking torque, thus granting precise control of the power dissipated by the braking resistor through duty cycle manipulation.

Furthermore, the implementation of a PID control strategy will then close the system's loop, allowing rapid and automatic adjustments of its characteristics in response to any variation of the working scenario.

The final model confirms the hypothesized behavior, providing a prototype for a new dynamic braking model which greatly reduces component deterioration and offers a precise and automated control on the testing procedure.

Contents

List of Figures

Chapter 1

Introduction

1.1 Purpose

In the world of electronics, one of the most common and efficient methods to drive motors is based on the Pulse-Width Modulation (PWM) technique. This involves creating a modulated square wave of given period and duty cycle thus creating a signal of a certain average voltage able to drive motors at a much more consistent and stable speed.

The work that was done has the aim of verifying the hypothesis that this same driving principle can be applied to a generator connected to a heating resistive element, effectively realizing a dynamic braking effect dependent on the duty cycle imposed on the transistors.

A testing motor was mechanically attached to a generator, itself electrically connected to a resistive heating element through a bank of 16 parallel MOSFET transistors, whose driving PWM signal was in turn controlled by the Arduino micro-controller.

After confirming a correct behavior of the working principle, a test bench was developed in order to be able to support several different keyed shaft motors and to offer a tunable braking torque.

1.2 Components

A diagram of the system is provided in figure 1.1.

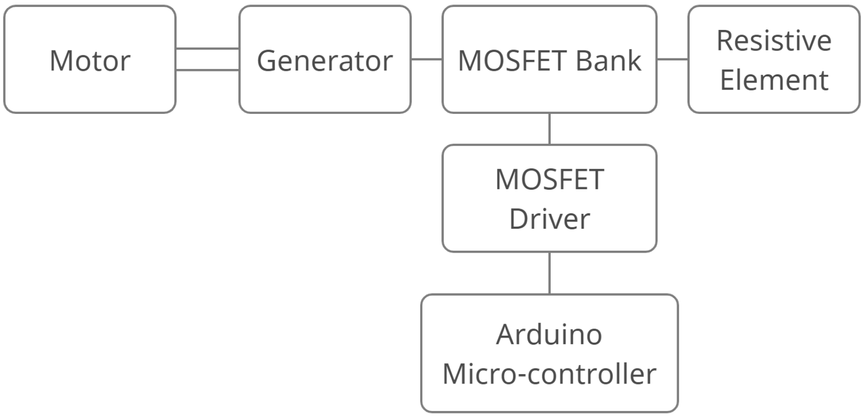

Figure 1.1: *Diagram of the system.*

The final system was composed of the following elements:

- Motor: an externally powered motor was used. Initially a speed and torque regulated motor was utilized, allowing for precise and specific testing of the system.
- Generator: an eolic 3-phase generator was used as a dynamometer capable of imposing a braking torque on the motor.
- Voltage Rectifier: a voltage rectifier was implemented in order to convert the AC output of the generator to direct current.
- MOSFET Bank: four groups of four transistors each were connected in parallel in between the generator and the heater. This configuration was implemented in order to withstand the high power output of the system. The MOSFET selected for this application was the IRFP460.
- Resistive Element: a 68 Ω 900 W braking resistor was used to dissipate the energy created by the generator.
- MOSFET Driver: a MIC4452 MOSFET driver was implemented in order to amplify the driving signal coming from the microcontroller in order to satisfy the transistors requirements.
- Arduino Micro-controller: an Arduino Uno microcontroller board was used for the generation of the signal and the tuning of parameters.

1.2.1 Motor

The engine used in this application is a three-phase alternating current machine AQCA 100S, with a test bench capable of control both in velocity and in torque. The characteristics of the motor are shown in table

P_n [kW]	n_n [RPM]	N_n [Nm]	Eff.	P.F.
4	1500	25.5	0.85	0.75

1.2.2 Generator

The main component of this assembly is a custom generator. It is based on two tri-phase eolic alternators mounted on the same keyed shaft. Even though they are branded Ducati Energia, they are fairly outdated, and as such their datasheet was unavailable, and consequently their rated characteristics unknown. The three phases of each generator were then connected to a couple of 3-phase bridge rectifier of mark DB 35-16, rated for up to 35 A and 1000 V_{rms}. A photograph of the generator is shown in figure 1.2.

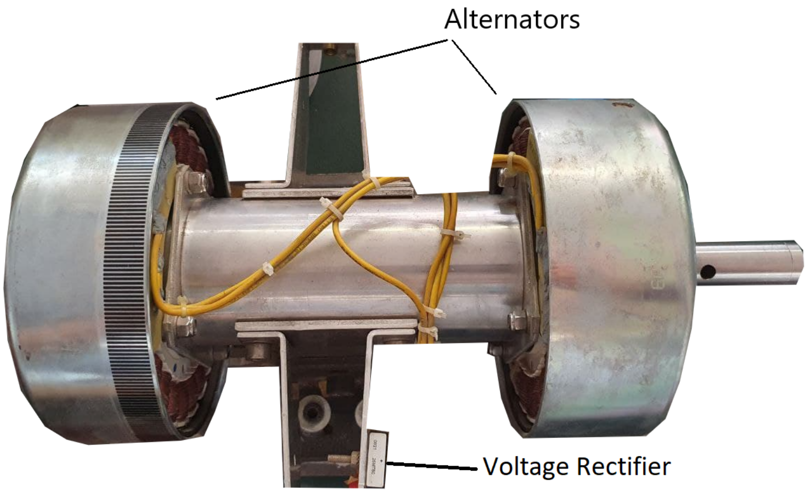

Figure 1.2: *Photograph of the used generator.*

.

1.2.3 Voltage Rectifier

A 3-phase full wave voltage rectifier was necessary to convert the generated alternating current signal to a more stable direct current one. The component of choice was the DB 35-16, rated for 45 A and 1000 V_{rms}. The rectifier was mounted to the metallic wings attached to the generator assembly. The schematic and forward characteristic of the component in question can be found in figure 1.3.

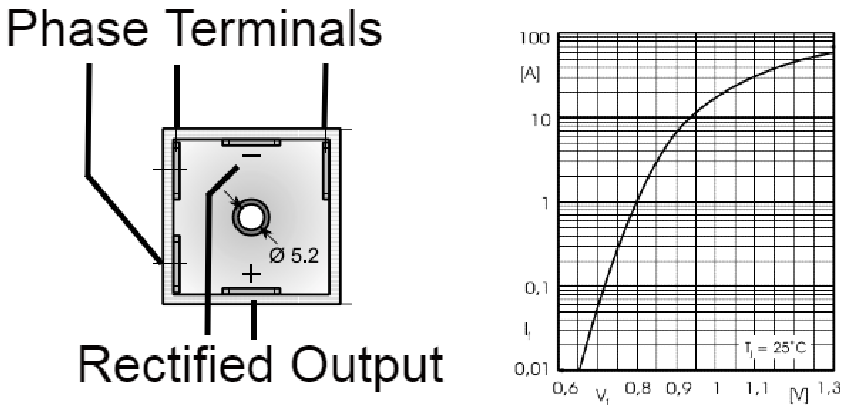

Figure 1.3: *On the left the schematic of the component. On the right its forward characteristic.*

1.2.4 Transistor Bank

A group of 16 parallel MOSFET transistors was implemented in order to withstand the high voltages that would be generated. The transistor of choice is an IRFP460, with the following characteristics, taken directly from its datasheet.

ABSOLUTE MAXIMUM RATINGS T_C = 25 °C, unless otherwise noted					
PARAMETER			**SYMBOL**	**LIMIT**	**UNIT**
Drain-Source Voltage			V_{DS}	500	V
Gate-Source Voltage			V_{GS}	± 20	
Continuous Drain Current	V_{GS} at 10 V	T_C = 25 °C	I_D	20	A
		T_C = 100 °C		13	
Pulsed Drain Current[a]			I_{DM}	80	
Linear Derating Factor				2.2	W/°C
Single Pulse Avalanche Energy[b]			E_{AS}	960	mJ
Repetitive Avalanche Current[a]			I_{AR}	20	A
Repetitive Avalanche Energy[a]			E_{AR}	28	mJ
Maximum Power Dissipation	T_C = 25 °C		P_D	280	W
Peak Diode Recovery dV/dt[c]			dV/dt	3.5	V/ns
Operating Junction and Storage Temperature Range			T_J, T_{stg}	- 55 to + 150	°C
Soldering Recommendations (Peak Temperature)	for 10 s			300[d]	
Mounting Torque	6-32 or M3 screw			10	lbf · in
				1.1	N · m

Figure 1.4: *The MOSFET characteristics.*

The selection of this component followed a careful examination for the one that would best suit our application, offering the best performance to cost ratio. Some values of note are found in the gate to source voltage V_{GS}, in the drain to source voltage V_{DS}, and in the maximum power dissipation P_D. The most important characteristic was the maximum power dissipation: at a value of 280W it meant that running the generator even at low RPM could incur in the overheating or the overloading of the MOSFETs. This problematic was resolved with the the assembly of 16 units in parallel, in order to share the power generated and to more efficiently dissipate heat. The transistors were mounted in groups of 4 on small stripboards, for ease of replacement in case of component damage, as shown in figure 1.5. A heat sink was attached to every transistor.

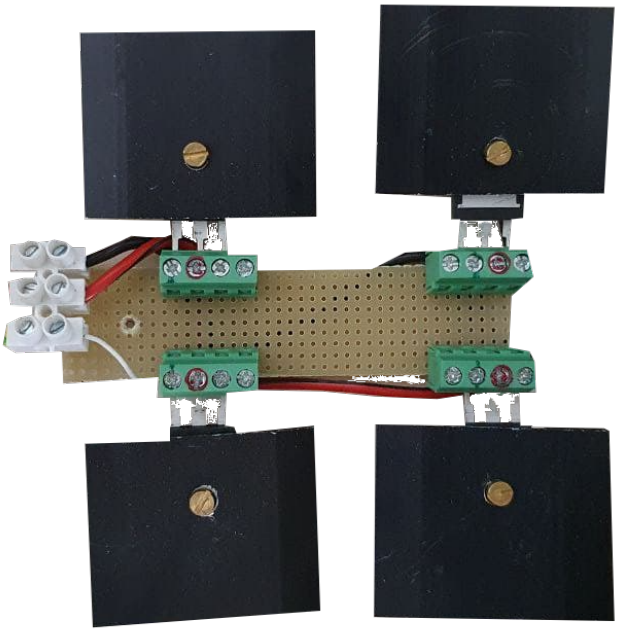

Figure 1.5: *A single bank of four MOSFETs with heat sinks.*

1.2.5 Resistive Element

The utilized braking resistor was marked MRIT 900-68R. Unfortunately, it again had been out of production for a couple of decades, but after a thorough research it was discovered to be similar in behavior to the NRIT IP20 2K2. This is a large protected braking resistor, purposely crafted with safety braking and test banks in mind. It is composed of an internal ceramic core around which a thermal wire is coiled. This inner core is surrounded by a metallic box modified for airflow. This construction is necessary in order to keep a safe distance from the possibly incandescent thermal wire. A photograph of the braking resistor is shown in figure 1.6.

Figure 1.6: *The braking resistor used, showing both the surrounding box and the inner thermal wire coil.*

1.2.6 MOSFET Driver

Since the required driving voltage for the selected transistors exceeded the available output voltage range of the microcontroller Arduino uno board, and given the large number of parallel transistors, a low side MOSFET driver was used to control the bank. In this system, a MIC4452 driver was selected, in view of its fast response and its very suitable characteristics. The main purpose of this chip is protection from current surges and electrostatic discharges coming from the transistors, while at the same time providing a sufficiently high voltage signal to drive the MOSFETs, maintaining the pulse modulation of the logic input unaltered.

The driver's schematic and characteristics can be found in figure 1.7.

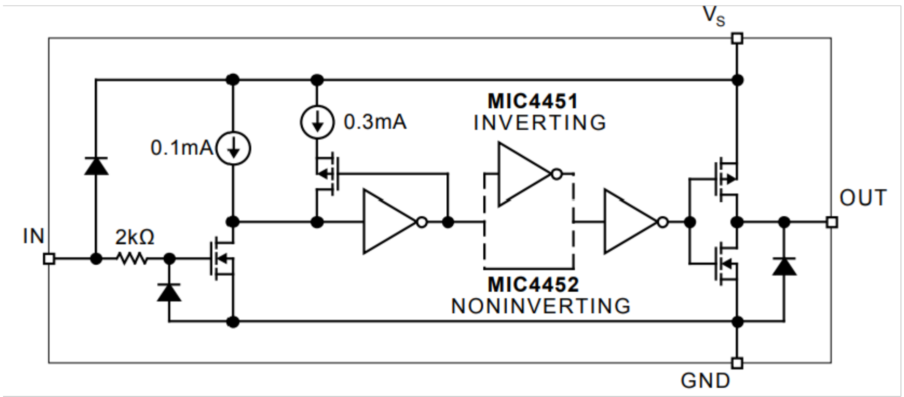

Symbol	Parameter	Condition	Min.	Typ.	Max.	Units
Input						
V_{IH}	Logic 1 Input Voltage		2.4	1.3		V
V_{IL}	Logic 0 Input Voltage			1.1	0.8	V
V_{IN}	Input Voltage Range		–5		V_S + .3	V
I_{IN}	Input Current	$0 \le V_{IN} \le V_S$	–10		10	µA
Output						
V_{OH}	High Output Voltage	See Figure 1	V_S –.025			V
V_{OL}	Low Output Voltage	See Figure 1			0.025	V
R_O	Output Resistance, Output High	I_{OUT} = 10mA, V_S = 18V		0.6	1.5	Ω
R_O	Output Resistance, Output Low	I_{OUT} = 10mA, V_S = 18V		0.8	1.5	Ω
I_{PK}	Peak Output Current	V_S = 18V (See Figure 6)		12		A
I_{DC}	Continuous Output Current		2			A
I_R	Latch-up Protection Withstand Reverse Current	Duty Cycle ≤ 2% $t \le 300\mu s$	>1500			mA
Switching Time(3)						
t_R	Rise Time	Test Figure 1, C_L = 15,000pF		20	40	ns
t_F	Fall Time	Test Figure 1, C_L = 15,000pF		24	50	ns
t_{D1}	Delay Time	Test Figure 1		25	50	ns
t_{D2}	Delay Time	Test Figure 1		40	60	ns
Power Supply						
I_S	Power Supply Current	V_{IN} = 3V V_{IN} = 0V		0.4 80	1.5 150	mA µA
V_S	Operating Input Voltage		4.5			V

Figure 1.7: *MIC4452 internal schematic and characteristics.*

1.2.7 Micro-controller Board

An Arduino UNO board was selected for this application. It is a microcontroller based on the ATmega328P processor. It features 14 digital pins and 6 analog pins, but most importantly it is capable of generating PWM signals with a frequency of either 490 Hz (on pins 3, 9, 10, 11) or 980 Hz (on pins 5, 6).

It is capable of serial transfer, thus making it possible to monitor and tune its behavior while running through a computer. It features its own IDE and a specific programming language, which is based strongly on C and C++.

Its maximum output voltage is however constrained at 5 V, hence the necessity for the transistor driver, which would amplify the digital signal. An image of the selected board can be found in figure 1.8.

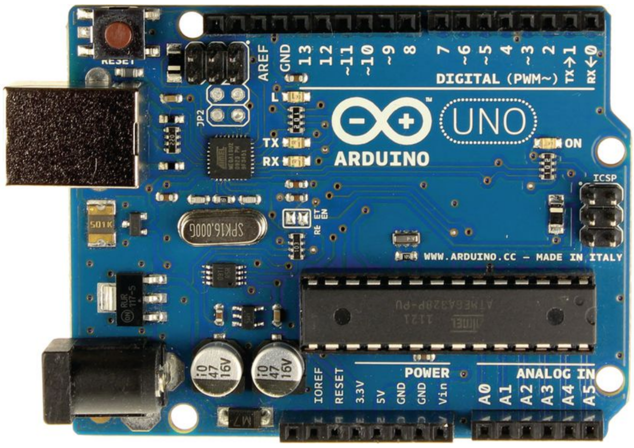

Figure 1.8: *The Arduino UNO microcontroller.*

.

Chapter 2

Theoretical Background

2.1 Dynamometers Overview

A dynamometer is a device capable of measuring the rotational speed and the torque of a motor. Furthermore it can be used as part of a test bench with the purpose of calibration and engine management. In this situation, it can be referred to as a brake dynamometer, and it is characterized by its variable resistance in regards to physical motion. By imposing a certain amount of braking torque on the motor, the device can gather information regarding the testing apparatus' characteristics.

There exist several different types of dynamometers, including Eddy Current, Powder, Hysteresis, Electric motor/generator, and hydraulic braking to name a few.

In this section a summary examination and comparison of the main motor braking techniques will be conducted.

2.1.1 Eddy Current Dynamometer

Whenever a conductor is moved through a given magnetic field, or whenever the magnetic field surrounding a stationary conductor varies, currents are induced in the body of the conductor. These currents, called eddy currents, will produce their own magnetic fields, which according to Lenz's Law, will have a direction opposite to the magnetic field that created them. The resistance that is therefore generated by the opposing magnetic fields is exploited as a method of braking rotating tools.

Eddy current braking makes use of the magnetic drag generated by the opposite facing magnetic fields to slow down any rotating conductor, such as a brake disk mounted onto a motor shaft.

This solution offers advantages in the absence of mechanical wear due to the absence of contact, and given the employment of electromagnets, the possibility to fine tune the braking magnetic field generated, depending on the current.

On the other hand, this methodology does incur in some problems, such as the physical heating of the conductor or its unsuitability to low speed applications, in view of the need of a quickly changing magnetic field or a quickly moving object. Moreover the impossibility of providing any holding torque forces the association of this technique to a mechanical one in certain scenarios. Figure 2.1 shows a representation of the interactions between the magnetic fields generated through eddy currents.

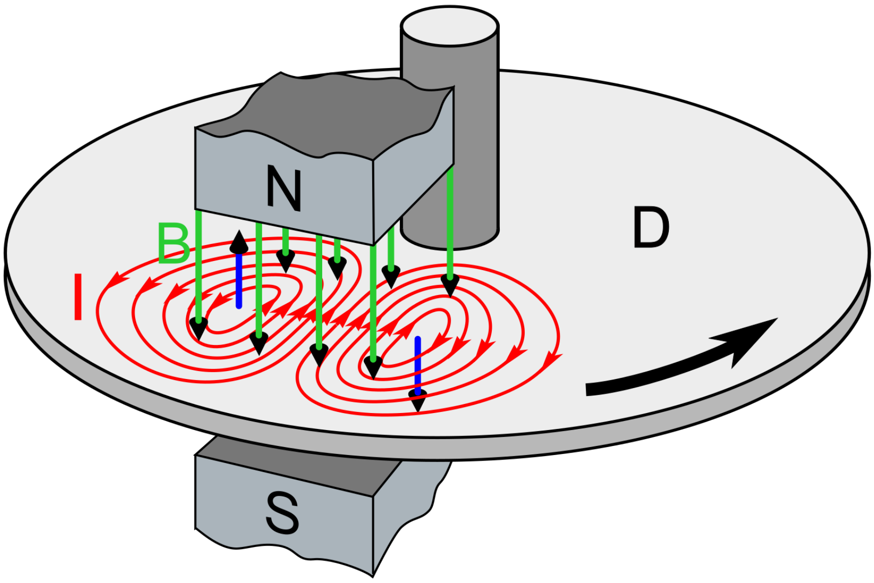

Figure 2.1: *Representation of the interactions between the magnetic fields generated through eddy currents.*

2.1.2 Powder Dynamometer

Working very similarly to the eddy current dynamometer, its powder variant makes use of a fine magnetic powder deposited in between the rotor and the coil. If an electrical current is sent through the coil, the generated magnetic field would excite the particles, changing their state from free flowing to completely solid at full excitation. The alignment of the powder with the magnetic field offers a smooth braking torque through friction, proportional to the current provided. As the rotor slows down, the drag generated does however erode the solidified powder.

This technique is more suited for low RPM high torque applications, given its inability to dissipate heat very efficiently. A distinguished advantage of this technique is the possibility to accurately control the braking torque right from the zero RPM starting conditions. This does however imply the presence of mechanical wear and the necessity of heat dissipation methods.

2.1.3 Hysteresis Braking

The hysteresis effect is based on two main components: a shaft assembly and a reticulated pole structure, fastened together but not in physical contact. The moment a magnetizing force is applied to the pole structure, the air gap between the two components becomes a flux field. In this way, the rotor is subject to a strong magnetic force which provides a braking action between the pole structure and the rotor.
A cross section of a hysteresis braking system is shown in figure 2.2 for a clearer visual understanding.

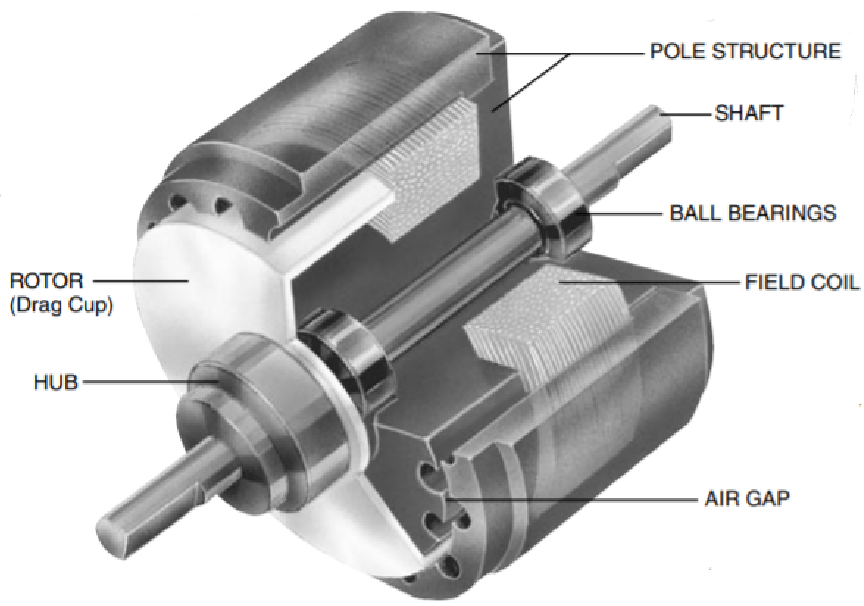

Figure 2.2: *Cross section of a hysteresis braking system*

This technique manages to avoid any sort of contact and therefore of friction of the components, thus increasing durability. Furthermore the braking force is directly proportional to the input current, making it easily and precisely adjustable. Moreover it can be applied immediately from a non moving condition.

The high currents required for the generation of the magnetic fields do however cause some amount of heat, which has to be dissipated as efficiently as possible to avoid disturbances to the electrical characteristics.

2.1.4 Generator Dynamic Braking

Most electric motors can function as generators. The concept of motor braking is based on a quick re-connection of the engine as a generator while it is still in rotation, rapidly stopping the motor and converting the moving body's kinetic energy into electrical energy to be dissipated.

This procedure is mainly performed in one of two ways:

- In Regenerative Braking the energy generated by the turning motor is stored in battery banks, effectively recuperating part of the energy spent to previously run the motor. Since the power supply system may not be capable of accepting the sudden and relatively high amount of energy this method could provide, usually a braking resistor is implemented in parallel, dissipating energy through heat.

- In Rheostatic Braking, most of the energy generated is then dissipated as heat by large braking resistors - large resistor coils turned on a ceramic core - connected to the armature terminals. This does however generate large amounts of heat and therefore requires a cooling system and thermal sensors, in order to avoid damaging the components.

Both methods are very efficient at high speeds, offering a lower wear on the components thanks to the lack of friction, a more profound control of the motor voltage, and a faster braking action in both AC and DC motors.

They do however lack when operating at low speeds, since the slower rotational speed implies a smaller generated energy and hence a reduced braking potential.

A circuit model of a motor working as a generator in a dynamic braking scenario is shown in figure 2.3.

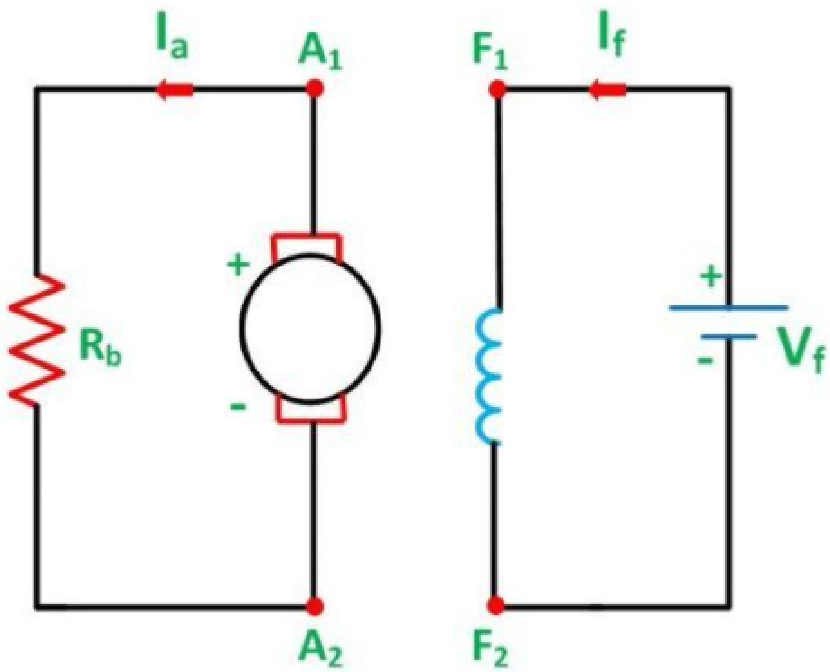

Figure 2.3: *Circuit model of a dynamic braking scenario.*

2.1.5 Hydraulic Braking

Hydraulic braking is one of the most commonly used method for slowing down rotating parts. It involves the pressing of a pedal or a lever to compress a chamber containing a fixed amount of braking liquid. This compression causes a pressure transfer from the level mechanism to the braking mechanism. Inside the latter, the constricted fluid is pushed against a padding element which in turn applies friction to a disk fused with the shaft.

The choice of hydraulic fluid is of paramount importance, since it must sustain very high temperatures without vaporizing, it must not be corrosive, and it has to be uncompressible.

This braking system is most commonly found in vehicles of all sorts because of its reliability and contained cost. It does however involve several mechanical components which increase the probability of failures occurring. Moreover it requires periodic maintenance considering the great friction it creates.

A depiction of the basic concept involving hydraulic braking is shown in figure 2.4.

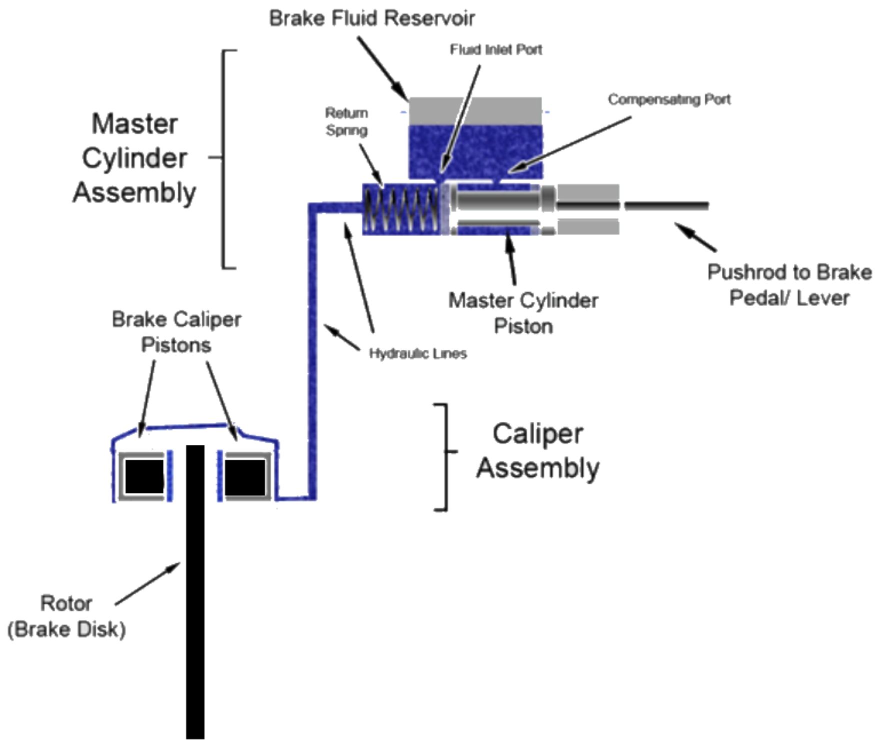

Figure 2.4: *Most commonly used hydraulic model.*

2.1.6 Proposed System Analysis

The dynamic braking technique adopted for this project is based on rheostatic braking, the only difference being that in our situation the motor is still alimented while the generator is connected to the braking resistance at a certain duty cycle and period, therefore it is subject to a certain braking torque.

Henceforth, a more in depth analysis of this method will be conducted in this section.

As previously stated, the dynamic braking method is based on the sudden usage of a motor as a generator after its working period. This causes the motor's kinetic energy to be converted into electrical energy at a specific efficiency rate, dependent on the internal frictions. The created energy is then dissipated through both the motor armature resistance and a secondary braking resistor. The purpose of this parallel resistance is to provide a restricted path for current to flow when the braking action occurs. Furthermore it helps restrict the magnitude of the current during braking so that it does not exceed the rated armature current.
Its main purpose is however to dissipate most of the created energy through heat dispersion.

The braking resistor's value has an effect on the braking capacity. Given a smaller resistance, more current will flow through it, thus absorbing the energy faster and offering a stronger braking effect. This will of course cause a faster generation of heat, possibly damaging to the resistor.

In the system being tested a similar situation takes place. The motor's shaft is connected with a key to the generator's shaft. This interconnection offers a mostly lossless transfer of kinetic energy from the provider to the receiver, both in terms of torque and in terms of rotational energy. The engine's power supply is external and as such it will be constant.

The generator will constantly act as a dynamic braking motor: as the motor causes it to rotate, some electrical voltage and current are created. These characteristics shall follow a linear behavior, increasing with the rotational speed. If the generator was disconnected from the rest of the system it would offer no resistance, since it could be approximated to an open circuit.

The generator is then connected through a bank of MOSFET transistors to a braking resistor, thus completing the circuit and offering a finely tunable braking effect, dependent on the duty cycle of the transistors, imposed by the microcontroller.

2.2 Three Phase Induction Motor

An electrical motor is a device used to convert power from electrical to mechanical. These machines are mainly distinguished in two categories: direct current (DC) motors, and alternating current (AC) motors.

The former follows a simpler design, based on two components, a commutator (a rotary part consisting of a cylinder composed of several segments, rotating with the armature to make alternating contact with the brushes), an armature (lengths of insulated wire coiled around a soft iron core), and a surrounding stator (an enclosure composed of two or more permanent magnets). There are several permutations of this machine, but the basic working principle is as follows: the internal armature, attached to the commutator, is excited with a current coming from the brushes through the commutator.In this way, an internal electromagnetic field is generated in the soft iron core. The external stator magnets cause a realignment due to the newly created electromagnetic field, which in turn causes the armature to rotate. As it is attached to the commutator it as well starts rotating. This causes the brushes to make contact with the opposite faces of the commutator, thus switching the polarity of the electromagnet created on the armature. In this way, the permanent stator magnets and the armature electromagnet are always misaligned, causing a continuous attraction and therefore a rotation. A representation of the direct current motor's working principle is shown in figure 2.5.

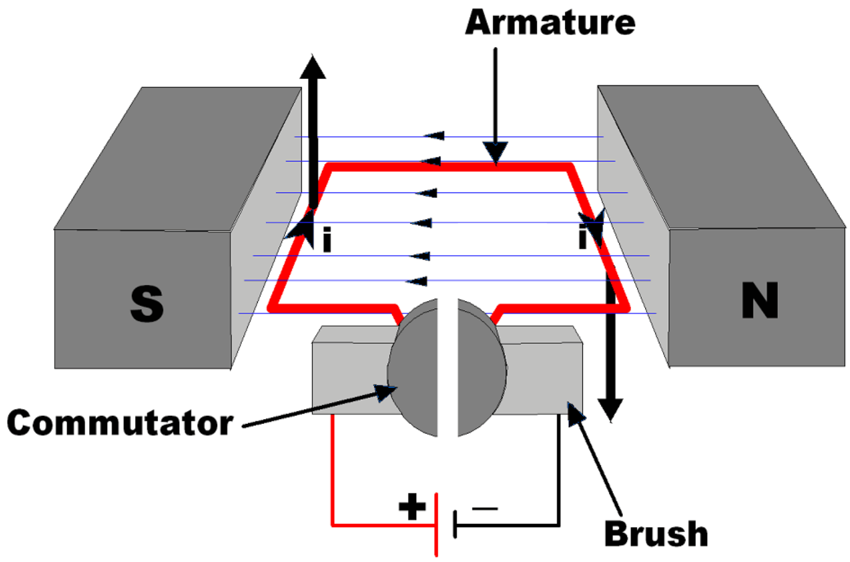

Figure 2.5: *Direct Current Motor working principle.*

The latter is instead composed of two main parts, a stator and a rotor. The stator consists of overlapping windings of insulated copper coil offset by 120° with respect to each other. It can be both internal and external to the rotor, which is composed of a cylindrical laminated core with parallel fitted conductors. The working principle is based on Faraday's law, which states that an electromagnetic force induced in a circuit is caused by a changing magnetic flux going through it. As the stator gets powered from a three-phase electrical source, each coil generates a magnetic field whose polarity changes as the alternating current oscillates. Since the three coils are shifted by 120°, their polarity is different on each time instant. This causes a rotating magnetic field to be generated. The rotor, in turn, subject to this RMF, feels an induced current, resulting in an opposing magnetic field according to Lenz's Law. The generated electromagnetic field tries to align its polarity against that of the stator field, resulting in a rotation and a torque applied to the shaft. A depiction of the 3 phase motor working principle can be found in figure 2.6.

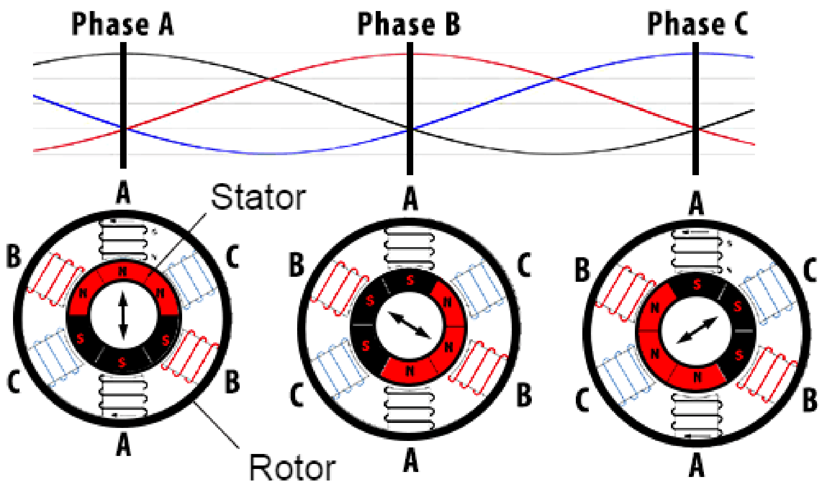

Figure 2.6: *Tri-phase Motor working principle.*

A three phase electrical machine can be used both as a motor and as a generator. In the second case, its function is related to that of three alternating current single phase generators, offset with respect to each other by 120°. In this way, the power generated will consist of three sinusoidal waves with a phase difference such that the effective output will be consistent.

Such a machine can be observed in two different configurations: a Delta connection or a Wye connection. In the former, the transformers are displaced in a triangular formation similar to the greek letter Δ, with three hot wires and an optional ground one, while in the latter the transformers are connected in a star formation, offering one more wire out of the system attached to the common terminal of the transformers, called the neutral line.

The star configuration enables the usage of both 208 Vac and 120 Vac lines, thus allowing for more flexibility. It does however require one more wire with respect to the delta connection, which can be very costly in long distance applications.

The delta configuration still finds its place in larger motors that do not require a neutral wire, or more commonly, in power transmission, given the reduced cost of one fewer line to route.

A representation of the two configurations can be found in figure 2.7.

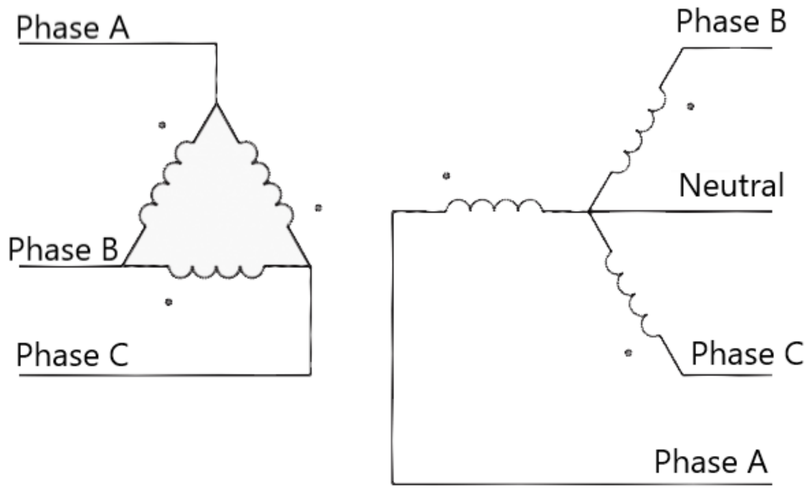

Figure 2.7: *The Delta and Wye configurations for 3-phase generators.*

2.2.1 Three Phase Electric Power

The electrical characteristics of the previously described scenario will be examined more thoroughly in this section.

Take three conductors, each carrying an alternating current (that is an electric current which follows a periodic pattern, reversing direction according to a given frequency) of a given and equal frequency and voltage amplitude. If these three conductors were displaced in such a way that their phases would be mutually distanced by 120°, a situation would arise where the voltage peaks of each conductor would occur with a constant periodicity, equidistant with respect to each other. This phase delay would then offer a more consistent power output. The produced line to line supply voltages V_{LL} will depend on the line to neutral voltage V_{LN} with the following relationship.

$$V_{LL} = V_{LN}\sqrt{3}$$

A graph representing the three different phases and their discrepancy is shown in figure 2.8.

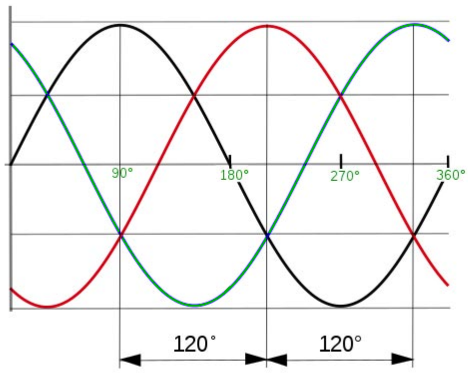

Figure 2.8: *Graph of the three phases in an AC configuration.*

A three phase system offers quite a few advantages over other electric power distribution systems. Since it requires only four cables to operate, its power transmission capability to material required ratio is very desirable. Furthermore the system can create a very finely tunable RMF, simplifying the design of electric motors thanks to the absence of a starting circuit.

2.2.2 Rectifier

In certain situations, the alternating current provided by the three phase electric power arrangement is inadequate for the application. If for instance direct current is required, the device known as rectifier can be employed. Its main purpose is in fact to convert an alternating current to a direct current. There are several different kinds of rectifiers, ranging from single phase half wave ones up to three phase full wave ones or voltage multiplying ones, each meant for different applications. In this section, we are going to be focusing on the three-phase bridge rectifier, also known as a full bridge rectifier.

In such a component, six diodes are implemented in order to cover as much as possible the three phases of the alternating current. Every time instant when a phase is negative one of the diodes is functioning to prevent the negative wave from reaching the output, thus permitting through only the positive values. In this manner, the input alternating current is in fact subject to an effect similar to an absolute value function. Furthermore, the full wave bridge rectifier implements a summing function whenever there are two different phases on the positive plane, effectively increasing the output voltage, as can be seen in figure 2.9.

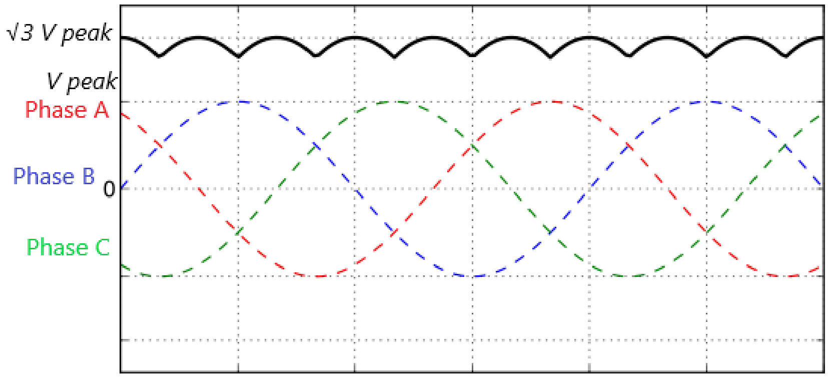

Figure 2.9: *Working behavior of a three phase full bridge rectifier.*

This device is often implemented together with a smoothing element such as a voltage regulator, in order to produce a steadier and even more consisted output voltage. This is usually done in situations where the DC load requires very little fluctuations in its input. Its basic function is not dissimilar to a voltage divider, which cuts the voltage at a value distant from the rippling.

2.3 Transistors

A transistor is an electronic device that can be used either as an amplifier of power and signals or as an electric switch. It stands at the base of modern technology, being employed in every possible application. It is mainly composed of a semiconductor material, most commonly silicon, and usually three terminals. One of these terminals is used to control the behavior of the other two. Their usage is so widespread and their development so fundamental that Gordon E. Moore made a prediction in this regard, stating that the number of transistors per silicon chip will double every year.

There exist a large number of different transistors, the main ones being MOSFETs, BJTs, and IGBTs.

2.3.1 MOSFET

The metal-oxide-semiconductor field-effect transistor (MOSFET) stems from the field-effect transistor typology, noteworthy in its functionality based on the controlled oxidation of a semiconductor material. It is by far the most common transistor in use.

It is composed of the semiconductor body to which are connected three pins: the gate pin, the drain pin, and the source pin. The gate is used as a control terminal: when a high enough voltage, that is a voltage higher than the threshold characteristic of the transistor, is applied between the gate and the source, the drain and the source, which act as a switch, close the circuit with the equivalent of a very small resistance.

MOSFETs are further divided into two categories, depletion mode and enhancement mode, their fundamental difference being in the required gate voltage. An enhancement mode transistor requires a positive V_{GS}, which will turn it on completely. On the other hand, a depletion mode MOSFET can accept either a positive or a negative gate voltage, but it never turns on completely.

Finally, another distinction can be made regarding this type of transistor. In particular they can be divided between N-type and P-type MOSFETS, the main difference being in their behavior as switches. In fact, the N-types will act as normally open switches, while the P-types will behave as normally closed ones. Their state will change as the gate receives a voltage higher than the necessary threshold $V_{GS,th}$.

The different electrical symbols used for the MOSFET variations are shown in figure 2.10.

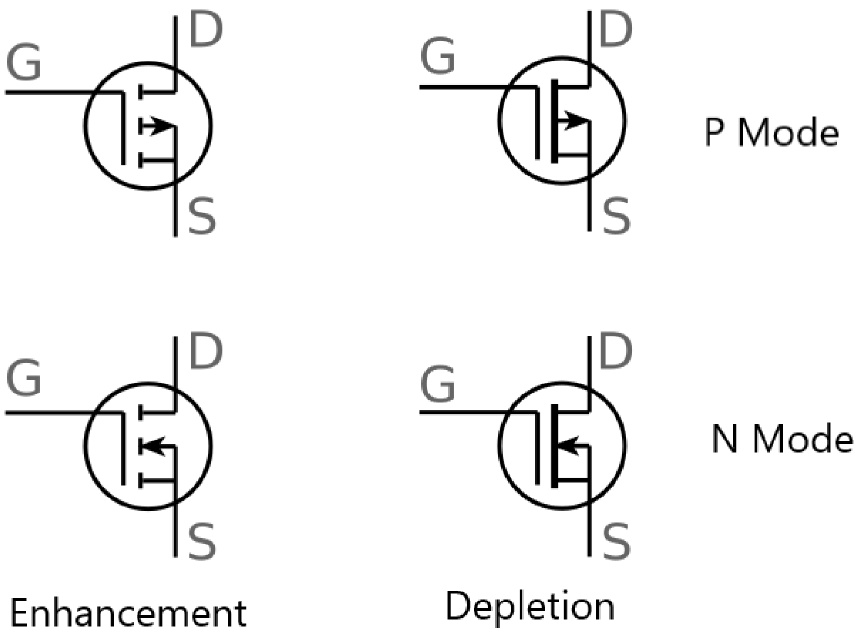

Figure 2.10: *Electrical symbols for the different MOSFET variations.*

Since this type of transistor can withstand high voltages and currents, heat dissipation becomes a real problem. In order to accommodate it, the drain pin is often connected to a metallic wing on top of the component, which allows for the attachment of a heat sink.

A particular type of MOSFET is the complementary MOSFET, or CMOS. It makes use of both a P and an N type MOSFETs symmetrically for logic functions. In principle it works as a NOT logic gate, but can be programmed to implement a wide variety of logic gates.

2.3.2 BJT

The bipolar junction transistor (BJT) is manufactured with three semiconductor regions, each one of these doped differently from the adjacent one (PNP or NPN). The three regions are known as Base, Collector, and Emitter. The BJT has two PN junctions (Base-Emitter and Base-Collector) that must be biased correctly through an external voltage signal in order for it to work correctly.

The two different types of BJT follow the same working principle, except they work with an opposite sign.

The working principle is based on the doping intensity of the different regions: the base region is in fact lightly dope, easily letting electrons in from the emitter region. As such, the free electrons in the base region move toward the collector region, where they are swept across it only to go into the overall circuit.

The operation of PNP and NPN transistors is very similar, except that the external bias voltages and current directions are reversed.

The switching speed it can support is however relatively slow .

The electronic symbols for BJTs can be seen in figure 2.11.

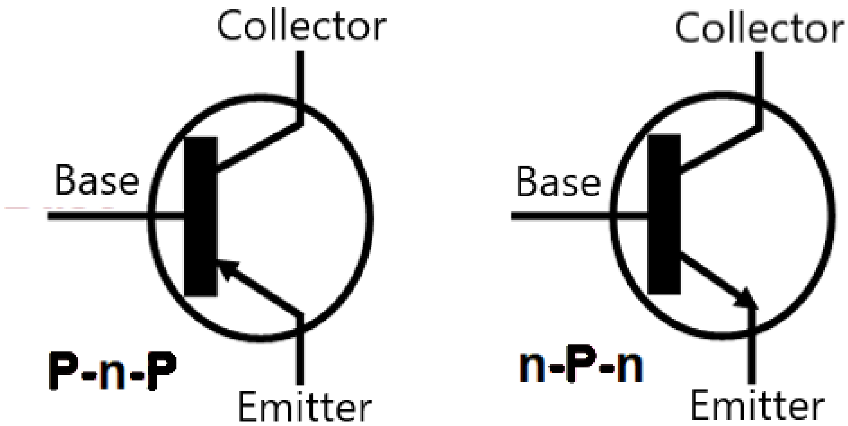

Figure 2.11: *Electric symbols for the BJT transistors.*

2.3.3 IGBT

The insulated-gate bipolar transistor (IGBT) is mainly used as an electronic switch, combining both the BJT and the FET in its design. It is composed of four layers of alternating doping controlled through a MOS structure.

The IGBT cell is similar in its construction to a MOSFET, the main difference being the N doped drain replaced by a P doped collector layer. It is therefore capable of withstanding much higher voltages and currents, while losing some switching speed and increasing greatly in cost.

2.3.4 Transistor Selection

In the required application, a careful transistor selection process was conducted.

The main characteristics that were considered follow:

- Switching Speed
- Output Voltage Range
- Input Voltage Range
- Maximum Power Dissipation
- Cost per unit

Since a pulse-width modulation technique would be implemented, the switching speed was a paramount characteristic, to be kept as high as possible. The frequency of the switching would need to withstand values as high as 980 Hz, which is the highest frequency the electrical board of choice could reach.

Another important value was the maximum voltage the transistor could withstand while working as a switch, that is the output voltage range. In our application, the generator was supposed to possibly reach up to 600 V. This would require surely a power transistor, and among those a fairly solid one. Furthermore, given the braking functionality that would be aimed for, the transistor would possibly be subject to high currents, although in the beginning there was not a possible range of such values.
Overall, the maximum power dissipation was taken into account, knowing that it would be a constricting factor, given the very nature of most power transistors.

The type of signal required for controlling the transistor was also considered in the selection process. Since the driving circuit would be at logic level, that is at very low voltages and currents, a low input range was necessary. Moreover, a voltage driver transistor was preferable over a current driven one.

Finally, the cost per unit was an impacting factor. The less expensive a component is the easier it is to replace in case of failure. Given the nature of this experiment, a cheaper kind of transistor was favored.

All the preceding characteristics led to the selection of a MOSFET as the transistor of choice for this application. In particular, the model IRFP460 seemed most appropriate among the more easily available ones. It offered a fairly high drain to source voltage at $V_{DS} = 500V$, a sufficiently high maximum for our application, given that the generator be kept at moderate RPM.

Its switching speed was in the order of nanoseconds, more than fast enough for the arduino Uno board.

The MOSFET was preferred for its ability to be driven by a voltage signal.

In this case, the threshold voltage necessary as input signal was $V_{GS} = 10V$, which proved problematic given the maximum voltage output of the arduino Uno board at 5 V. The simplest and most efficient solution proved to be implementing a transistor driver between the arduino and the MOSFET, which would receive the 5 V PWM signal from the board and output that same PWM signal boosted at 12 V, while at the same time providing a protection circuit for the microprocessor.

The main drawback of this choice was found in the maximum power dissipation $P_d = 280W$, a value definitely insufficient for an application where the generator would surely turn at moderate speeds. The implemented solution was to set up sixteen MOSFETs in parallel, in order to share the current output and to more easily dissipate the power generated.

The main characteristics of the selected MOSFET can be found in figure 2.12.

PRODUCT SUMMARY		
V_{DS} (V)	500	
$R_{DS(on)}$ (Ω)	V_{GS} = 10 V	0.27
Q_g (Max.) (nC)	210	
Q_{gs} (nC)	29	
Q_{gd} (nC)	110	
Configuration	Single	

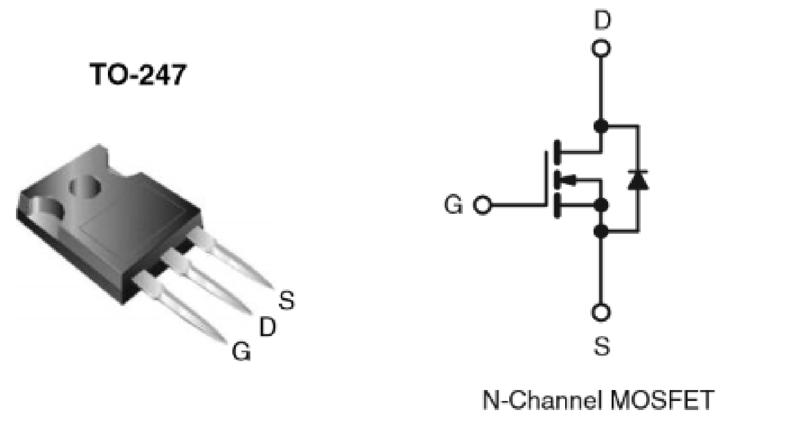

Figure 2.12: Characteristics of the chosen MOSFET.

2.4 Pulse-Width Modulation Technique

The pulse-width modulation (PWM) technique is a method often employed in applications where a high power output is necessary for extended periods of time. It is used to reduce the average power delivered by a signal by controlling a switch between the supply and the load and switching it on and off at a very fast rate. This grants the possibility to tune the percentage of time the switch is kept closed, known as the Duty Cycle, thus determining the amount of power to be let through.

The PWM is based on two parameters, the duty cycle and the period.

The latter is the frequency at which the power supply must switch. It can vary greatly according to the required application. This value has to be chosen carefully, as to affect the load performance as little as possible. For instance, if a light bulb were powered with a PWM signal at a frequency of 1 Hz, the length of time during which it would be turned off would be far too noticeable.

The former is the percentage of time of the period during which the switch will stay closed. This effectively dictates how much power will be let through to the load. A low duty cycle will entail a low power throughput.

This technique offers a few advantages, the most important of which is the very small power loss in the switching action. Since an open switch can be represented as an open circuit, the current losses are at a minimum. In a similar way, when the hypothetical switch is closed the voltage drop across it tends to zero.

The simplest method which can be used to generate a PWM signal entails the use of a sawtooth waveform and a comparator: the reference signal is compared to the sawtooth waveform and as the first is higher than the second, the PWM signal is set to high, otherwise it is set to low.

A graphical representation of the PWM technique at different duty cycles can be found in figure 2.13.

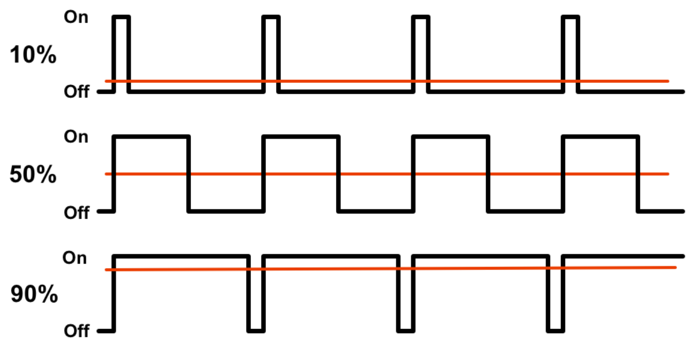

Figure 2.13: *Pulse-width modulation at different duty cycles.*

2.4.1 Arduino Implementation

The arduino Uno microcontroller is unable to output true analog signals, in the sense that the board does not have a driver necessary to create the voltage. In order to compensate, the PWM technique is used. The digital control takes care of creating a square wave which is switched on and off at precise frequencies and duty cycles, thus emulating an analog behavior.

The function *void analogWrite(pin, value)* takes as argument a digital pin and an integer number ranging from 0 up to 255, where 0 equals a duty cycle of 0% and 255 equals to a duty cycle of 100%.

Only a few selected pins are capable of supplying the PWM behavior. In the arduino Uno board, those are the digital pins 3, 5, 6, 9, 10 and 11. Most of the pins operate at a frequency of 980 Hz but the connectors 5 and 6 operate at a reduced frequency of 490 Hz because of internal interactions in the board.

Finally, if a different frequency is required of the arduino board, it is possible to change the internal timings through software means, although this can cause problems with other timing functions. This operation may prove necessary if the application requires a very specific frequency.

2.5 PID Control

The proportional-integrative-derivative (PID) control is a method mostly used to drive motors which implements a feedback loop to continuously modify the control parameters, calculating the error value and applying a correction through three terms, a proportional, an integral, and a derivative one. The error term is calculated as the difference between the desired value (known as Set Point) and the measured value (Known as Process Variable), the latter of which is read by means of a sensor and fed back to the system.

A generic schematic of a PID controller can be found in figure 2.14.

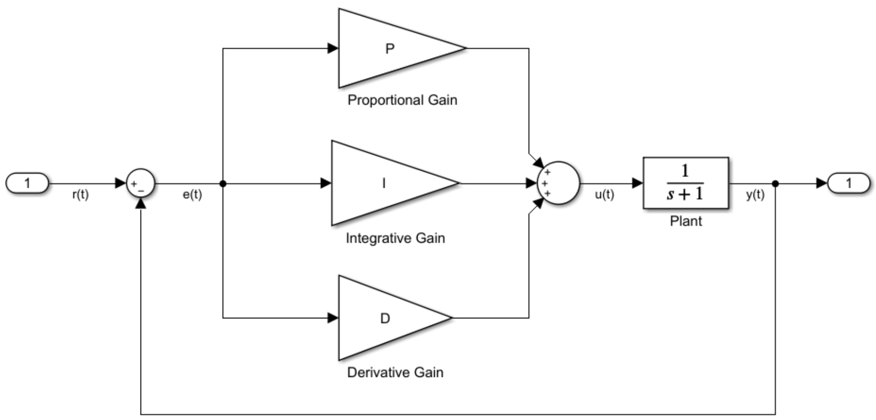

Figure 2.14: *Schematic of a PID controller.*

The three PID variables are modified in such a way that an automated control can be carried out on the output signal, accounting for external disturbances and counterbalancing their influence.

The controller aims to minimize the error which develops over time by imposing adjustments on the control variable *u(t)*, in order to have a stable and consistent output $y(t) = e(t) + r(t)$, where *r(t)* is the reference signal.

The different gains have different impacts on the system, as follow:

- The Proportional Gain takes its name from its relation with the error term. The larger the error the higher the K_P gain will be. Employing only this kind of correction will result in the generation of an error between the desired value and the measured one, since it requires an error itself.

- The Integral Gain factor works as a memory element, taking into account past values of the error and integrating them over time. As the error gets eliminated by the compensating factor K_I, the integral term itself will stop increasing.

- The Derivative Term tries to estimate the behavior of the error in future time instants, based on its current rate of change. The faster this value, the greater the gain effect K_D

The three PID terms have to be carefully balanced, differently for each application of this control method. This process is known as tuning. It allows by trial and error to find the best values for the gain factors which allow for a stable control of the system. Approximate values can be used as starting factors, but they have to be further refined by purposely disturbing the system and observing its behavior with different variables. The final function of the controlled input derived from a PID control system results in the following equation:

$$u(t) = e(t) \cdot K_P + K_i \int_0^t e(\tau) \cdot d\tau + K_d \frac{de(t)}{dt}$$

where u(t) is the control variable, K_p is the proportional gain, e(t) is the error value, K_i is the integral gain, de(t) is the change of error over time, and K_d is the derivative gain.

Chapter 3

System Development

The first step in the work that was accomplished entailed having a clear and straightforward understanding of the working principle of the complete system. The designed project involved a number of components:

- A motor provided with a test bench, controllable both in torque and in velocity
- A generator composed of a couple of eolic transformers mechanically attached to the same shaft.
- A braking resistor, which basically consists of a conducting coil wrapped around a ceramic core, the whole assembly surrounded by a steel case.
- A voltage rectifier, an electrical component capable of converting the generated alternating current to a more stable direct current.
- A transistor element capable of supporting a PWM controlling signal.
- A controller, in our case an electrical board Arduino Uno.

The starting idea involved the motor being attached to the same shaft by means of a flexible connector, in order to avoid any small discrepancy in the alignment of the two machines. An image of the aforementioned setup is shown in figure 3.1. The final mounting setup involved four 16 mm threaded bolts clamped to the workbench and running through holes in the mounting platform of the generator. By using bolts, washers, and spring washers, a very fine tuning of the generator's position was achievable, thus reaching the exact height of the motor's shaft. The spring washers were implemented for vibration dampening. The motor on the other hand was simply clamped to the workbench.

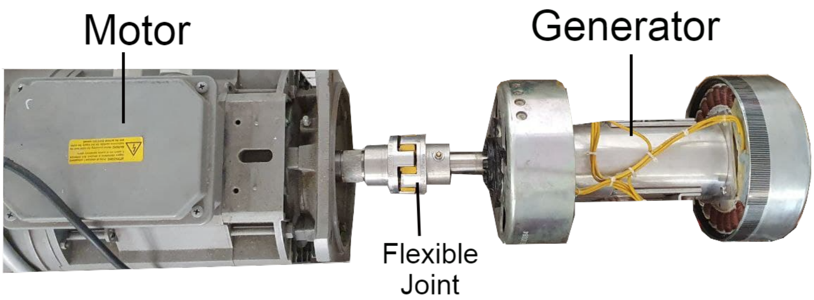

Figure 3.1: *The setup of the motor connected to the generator through a flexible joint.*

The motor would be controlled in speed, while its available torque would be set as high as possible, to allow for a clean performance.

As the generator would receive a turning torque, some amount of electrical power would be generated at its output. The three phases coming from the machine would need to be rectified, an operation undertaken by the voltage regulator. In the beginning, only one of the two generators would be connected, in order to first thoroughly understand its inner workings.

The direct current generated by the voltage regulator would then be fed into the transistor through a protection circuit based on power electronics. This would of course need to be implemented for our particular application.
The transistor would be controlled by a pulse-width modulated signal coming from a programmable microcontroller board. The one of choice for this application was the Arduino Uno.

The power accumulated by the generator would then have to be dissipated in some way in order to provide the braking effect. This was the braking resistor's job: according to the selected duty cycle, a certain amount of power would effectively be able to run through the transistor into the resistor, being transformed into heat and thus dissipated. This phenomenon has a greater magnitude at higher speeds, since then a larger voltage would be generated and thus more energy would flow into the resistor. However this could cause overheating of the resistive element. Therefore some care is needed in not overloading the system and allowing time for cooling off. Moreover, a lower resistance offer a faster and stronger braking force, at the cost of even more heat being generated. The resistor does need a very high power rating in order to safely accomplish this job.

At this point, the overall hypothesized system was laid out, and the testing procedure could be started.

3.1 Proof of concept

Approaching the development of this system, the first necessary thing was to plot the characteristic function of the generator in use. Through such a graph, one could learn the behavior of the component in different working conditions. This is a paramount bit of information while working with electrical machines. Unfortunately, the generator in question was an ancient piece of technology, offering no component number or immediate characteristics table. A further research was conducted, contacting Ducati Energia, the producer of the machine. They however were not able to offer any assistance, as the generator had been out of production for 20 years.

As such, the maximum characteristics of the machine were unknown, as well as any ratings. Any further work was therefore conducted in the dark, and the appropriate precautions were followed in order to avoid damaging the machines or the components.

3.1.1 Component Testing

In the beginning, the correct theoretical functioning of the alternators was investigated. Each phase of the generator was connected to an oscilloscope: through this test, the expected behavior would involve the three sinusoidal waves representative of the phases delayed with respect to each other by 120°. After the interconnection was established, through the use of crocodile clips connected individually to the three outputs of the alternators, the generator's rotor was turned by hand. The oscilloscope's display correctly showed the three offset phases, whose magnitude would increase as expected as the turning speed grew higher and decrease inversely, as can be seen in figure 3.2.

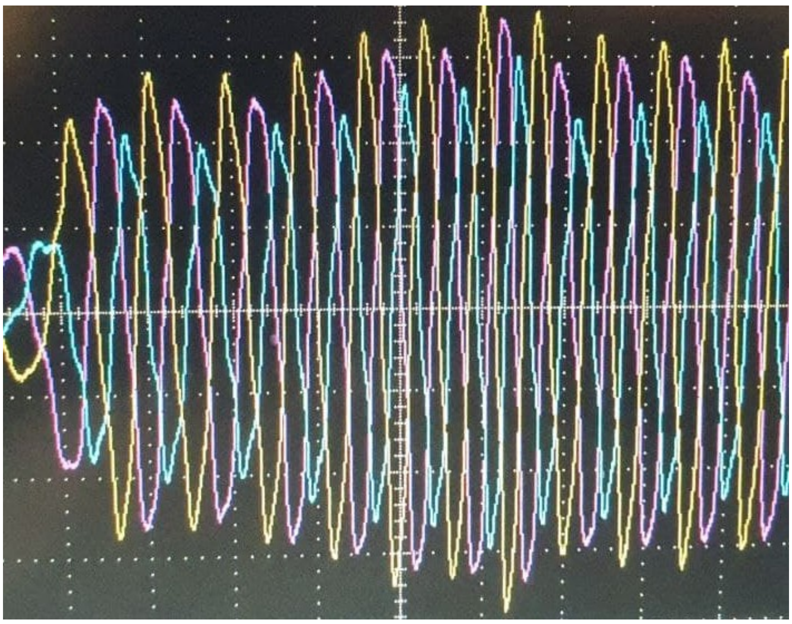

Figure 3.2: *The oscilloscope screen showing the three phases of the generator after hand turning.*

Having ascertained the health of this main component, the next step was checking the output of the voltage regulator. The expected behavior would entail a steady direct current voltage, proportional to the alternating current voltage through the approximation $V_{out} = V_s\sqrt{3}$, where V_{out} is the output voltage of the regulator and V_s is the input maximum line to line voltage. After connecting the three phases of the machine to the inputs of the regulator, the latter's DC voltage output was measured by means of both an oscilloscope and a multimeter, and it was found to be in line with the phases amplitudes.

Since a correct DC signal was now available, the next step would be to understand if the characteristic behavior of the generator was in line with the driving motor. The expected behavior would be a graph were the velocity of rotation and the output voltage rose with a linear dependence on each other, thus creating a straight line as shown in figure 3.3.

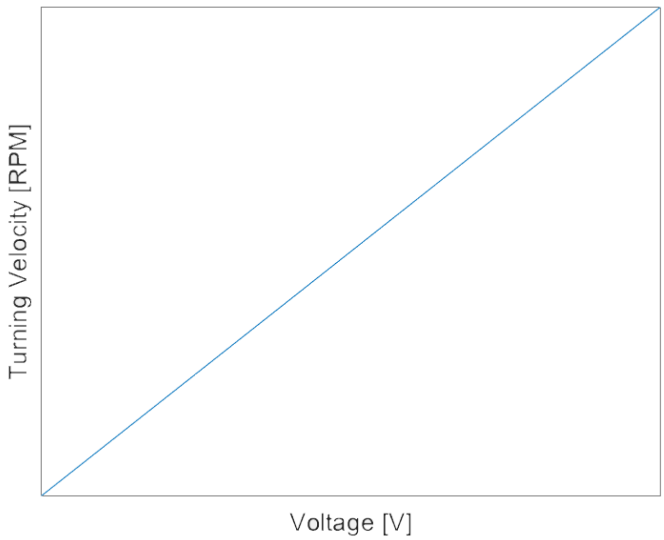

Figure 3.3: *The characteristic graph of a generator's expected behavior.*

In order to check this behavior, a multimeter was connected to the output of the regulator, and the voltage was measured at different velocities imposed by the motor on the generator. What resulted followed the expected bearing, accommodating for small non idealities, as can be seen in figure 3.4.

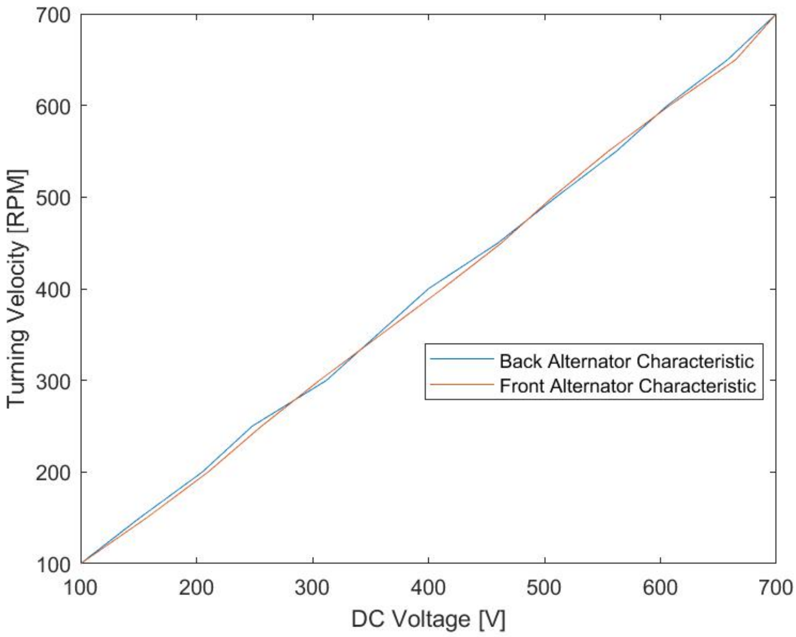

Figure 3.4: *Measured characteristic of the generator.*

The test was conducted on both the alternators. The measured behavior was found to be very similar, within an acceptable degree of tolerance.

3.1.2 Hypothesis Testing

The next step in the testing of the assembly had the purpose of understanding the behavior of the generator as its rectified output would be connected to the braking resistor. As the rectifier's output would be connected to the resistance, the system's output would effectively be connected to a load, hence requiring the generated electrical power to be dissipated as heat in the resistive element. The theoretical behavior would then show a slowing effect on the generator and by consequence the driving motor.

The interconnection was constructed by means of a simple normally open switch. The mechanical component was placed between the output of the voltage rectifier and the input of the braking resistor, thus effectively controlling the attachment of a load to the system. The current system is described by the following diagram (3.5).

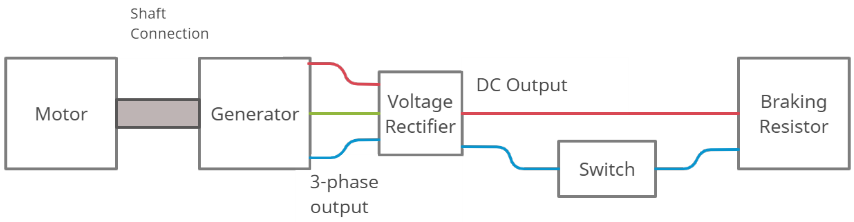

Figure 3.5: *A diagram of the system with a switch connected to the braking resistor.*

As expected, as the switch was closed, the motor's speed would drastically reduce and the braking resistor's coil would start heating up from the electrical power dissipation, thus confirming the behavioral expectations.

Further tests were conducted by tuning the torque provided by the motor. Under a certain parameter, the machine would be unable to turn the generator, being completely stopped by the braking force applied through the resistor.

This behavior is due to the amount of current going through the resistance: since the current is proportional to the mechanical torque, the more of the former implied a larger amount of the latter. A faster rotating alternator would then create higher voltage and current, thus involving a stronger braking force.

Oppositely, at low RPM, the effectiveness of the system is quite reduced, since the generated power is relatively small.

3.1.3 Hardware Testing

Since the system was now functional and the working hypothesis confirmed, the successive step would be building the power electronics required for interfacing the microcontroller Arduino to the power MOSFET and by consequence the alternator. Of course this connection could not be immediate and direct, but it would require some circuitry to boost the controlling signal coming from the electrical board and to protect the microcontroller itself.

In the beginning, the developed circuit was tested on a simple LED diode connected to an external power supply. This was done to ascertain the correct behavior of the system before working with high voltages and possibly damaging important components. The circuit was assembled on a breadboard, the schematic can be found in figure 3.6.

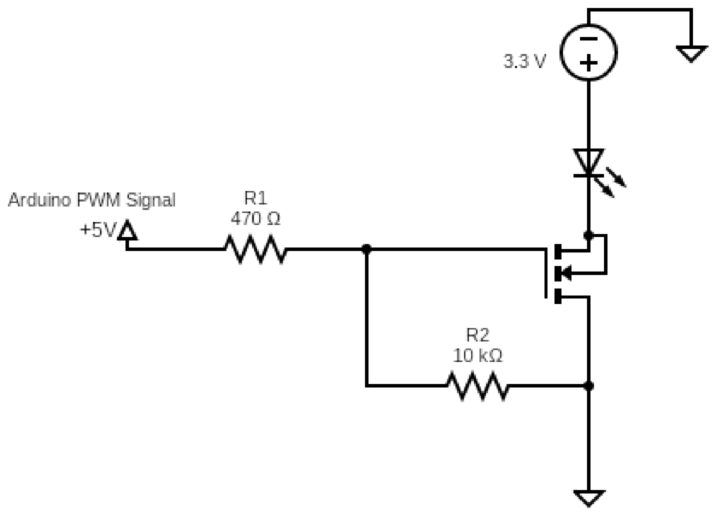

Figure 3.6: *The circuit developed for testing the PWM signal with an LED diode.*

.

The purpose of the resistance R1 is to limit the reverse current that will flow through the system due to the parasitic effect of the MOSFET's gate capacitance. The resistor R2 is used as a pull-down resistance, whose main purpose is to reset the transistor's status after the controlling signal is turned low.

As the duty cycle was modulated through the software the LED brightness would decrease or increase, following the behavior imposed on the PWM signal. This signified that the system was correctly working, and therefore the circuit could be further developed for the actual application, as can be seen in figure 3.7.

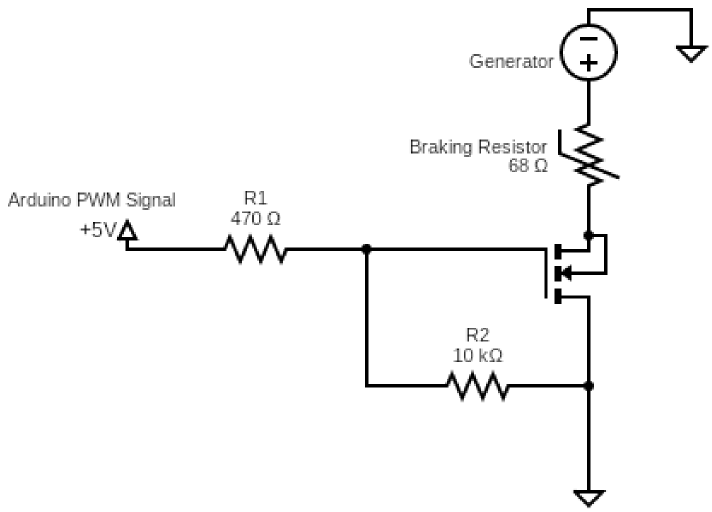

Figure 3.7: *Circuit developed for microcontroller protection*

Since the Arduino board could only provide up to 5 V and the MOSFET required a $V_{GS} = 10V$ the behavior of this system was prone to instabilities. Knowing this, the model was soldered on a stripboard and tested with a single transistor component at a reduced and controlled RPM.

The behavior was found to be compliant with the expectations, as with the tuning of the pulse width modulated signal's duty cycle, so would change the speed of the motor turning the generator, and therefore the slowing torque supplied by the braking resistor.

Furthermore the correctness of the wave was acknowledged by connecting a multimeter in different instances both at the output of the arduino and at the output of the MOSFET: in both cases, the picked up signal was coincident with the software imposed characteristics, following any changes applied to them.

3.2 Final System Design

As the hypothesized behavior of the system was now confirmed, the final model development was started.

In order to solve the insufficient output of the arduino with respect to the required V_{GS}, a possible circuit with a couple of cascading MOSFETs was theorized. The first and smaller transistor, connected to the board, would have a lower V_{GS}, thus being controllable directly by the Arduino. It would then have its Drain terminal connected to the Gate terminal of the power MOSFET, thus being able to control its behavior thanks to an external power supply of 12 V DC. This solution would require a further deepening of the previously constructed circuit, as shown in figure 3.8.

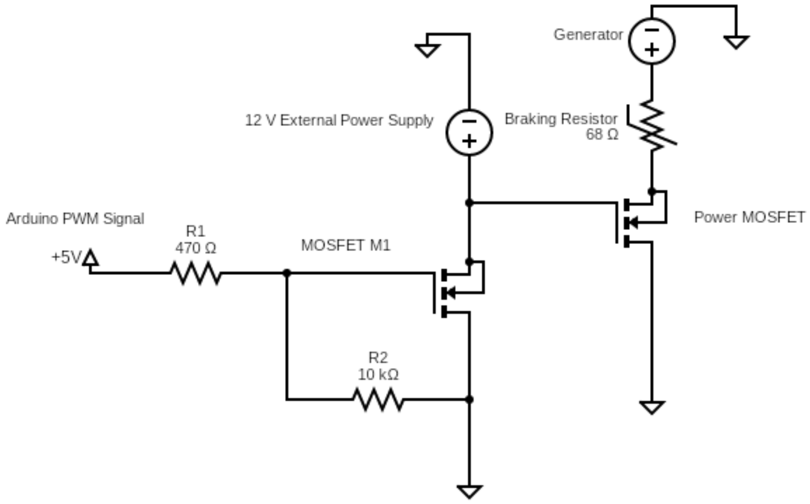

Figure 3.8: *The circuit developed with two cascading MOSFETs.*

This circuit was then assembled on a breadboard and tested. Its characteristics were checked both at the transistor M1 and at the power MOSFET's Drain terminal, and while the square wave was found to be correct at the first junction, it was unclean and disturbed at the second one. Furthermore, the power MOSFET would quickly overheat even if attached to a heat sink, resulting in damage to the component.

This approach was then abandoned for a different solution, that is the implementation of a low-side MOSFET gate driver. Such a component would implement the protection circuit while at the same time boosting the controlling signal from the standard 5V to the necessary V_{GS}. At the same time, it could accept any logic input, maintaining the PWM nature of the arduino signal. Finally it would reduce the PCB area requirements, while simplifying the product design.

The component of choice was a MIC4452 non inverting MOSFET driver, whose functional diagram can be found in figure 3.9.

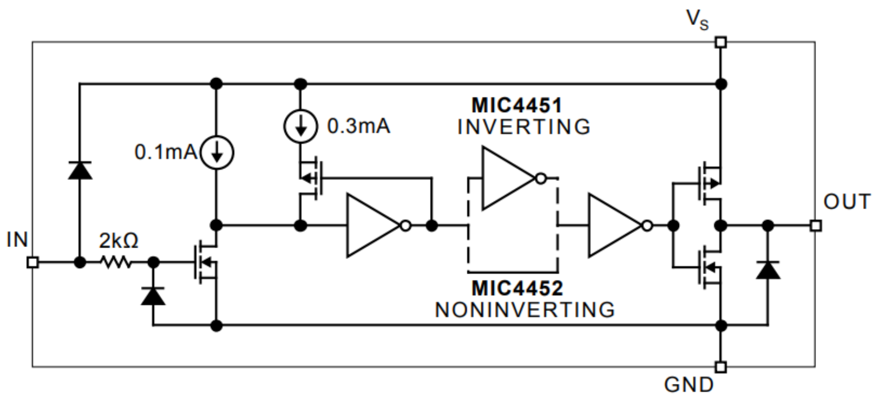

Figure 3.9: *Functional diagram of the MIC4452.*

By providing a $V_s = 12V$ DC power supply, which would then be used to power the Arduino board as well, the driver would be capable of boosting the input logic signal from 5 V to a higher value, that is $V_s - .025$, enough to respect the V_{GS} requirement of the power MOSFET. Moreover, given the very fast switching time of the driver, in the order of nanoseconds, the pulse-width modulated signal coming from the arduino would be left untouched in frequency and duty cycle. The electrical characteristics of the MOSFET driver can be found in figure 3.10.

Symbol	Parameter	Condition	Min.	Typ.	Max.	Units
Input						
V_{IH}	Logic 1 Input Voltage		2.4	1.3		V
V_{IL}	Logic 0 Input Voltage			1.1	0.8	V
V_{IN}	Input Voltage Range		–5		V_S + .3	V
I_{IN}	Input Current	$0 \le V_{IN} \le V_S$	–10		10	µA
Output						
V_{OH}	High Output Voltage	See Figure 1	V_S –.025			V
V_{OL}	Low Output Voltage	See Figure 1			0.025	V
R_O	Output Resistance, Output High	I_{OUT} = 10mA, V_S = 18V		0.6	1.5	Ω
R_O	Output Resistance, Output Low	I_{OUT} = 10mA, V_S = 18V		0.8	1.5	Ω
I_{PK}	Peak Output Current	V_S = 18V (See Figure 6)		12		A
I_{DC}	Continuous Output Current		2			A
I_R	Latch-up Protection Withstand Reverse Current	Duty Cycle ≤ 2% t ≤ 300µs	>1500			mA
Switching Time(3)						
t_R	Rise Time	Test Figure 1, C_L = 15,000pF		20	40	ns
t_F	Fall Time	Test Figure 1, C_L = 15,000pF		24	50	ns
t_{D1}	Delay Time	Test Figure 1		25	50	ns
t_{D2}	Delay Time	Test Figure 1		40	60	ns
Power Supply						
I_S	Power Supply Current	V_{IN} = 3V V_{IN} = 0V		0.4 80	1.5 150	mA µA
V_S	Operating Input Voltage		4.5			V

Figure 3.10: *MIC4452 driver electrical characteristics.*

Hence, the updated circuit was composed of the arduino microcontroller, the MOSFET driver, and a single transistor with a heat sink. The introduction of the driver simplified greatly the schematic with respect to the previous layout, as can be clearly seen in figure 3.11.

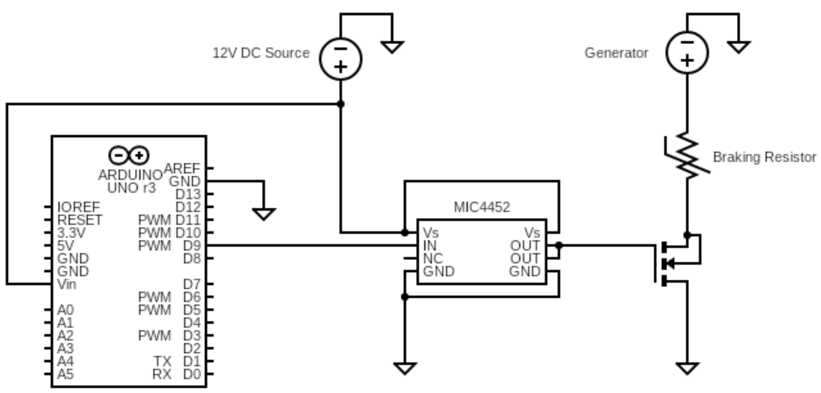

Figure 3.11: *The circuit with the transistor driver implementation.*

After conducting some testing procedure, the system was found to be working perfectly. In particular, as the duty cycle was modulated, the braking torque imposed on the motor would change accordingly. This circuit design however allowed only for small rotational velocities, since the maximum power dissipated by one transistor is $P_D = 280W$. Therefore the system could only be safely tested up to approximately 200 rounds per minute, since at that velocity the current generated approached 1.5 A at 100% duty cycle. This would result, using the subsequent formula, in a generated power $P = 300W$ which could cause damages in the component.

In order to surmount this problem, the solution that was pursued involved the creation of four parallel banks each composed of four parallel MOSFETs. The four groups would then be connected in parallel to the system, in place of a single transistor. In this way, the system could be able to handle much larger quantities of power, since the current generated would be divided among all the parallel branches, severely decreasing the power each MOSFET would have to withstand. Moreover, each and every transistor was supplied with a heat sink, to further help with the dissipation of the energy passing through it.

An image of a bank of four parallel MOSFETs can be found in figure 3.12.

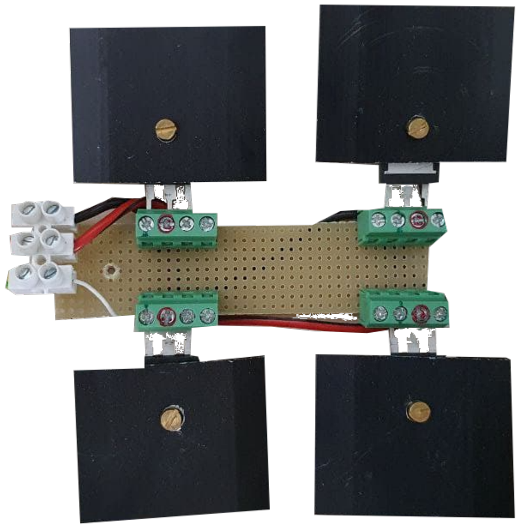

Figure 3.12: *One of four parallel banks of transistors.*

The schematic of a single bank's connections can be found in figure 3.13.

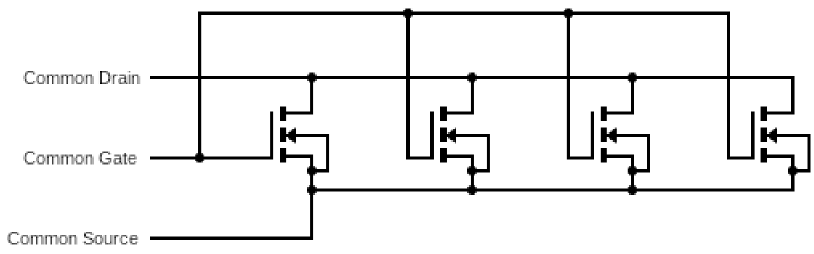

Figure 3.13: *The schematic of a single bank of four transistors.*

Four of these groups were then assembled on a single stripboard, and their common outputs were placed in parallel with each other, thus creating a bank of 16 parallel MOSFETs.

The distinction in four groups was implemented for ease of replacement in case of component damage. In the same spirit, each MOSFET was not soldered to the stripboard, but was attached to it by means of a terminal block.

The developed system was tested thoroughly and it was found to be working very well, withstanding higher RPM while maintaining a tolerable working temperature. The splitting of the current among all the different transistors allowed the system to withstand higher velocities without the risk of burning a component.

The schematic of the final system is shown in figure 3.14.

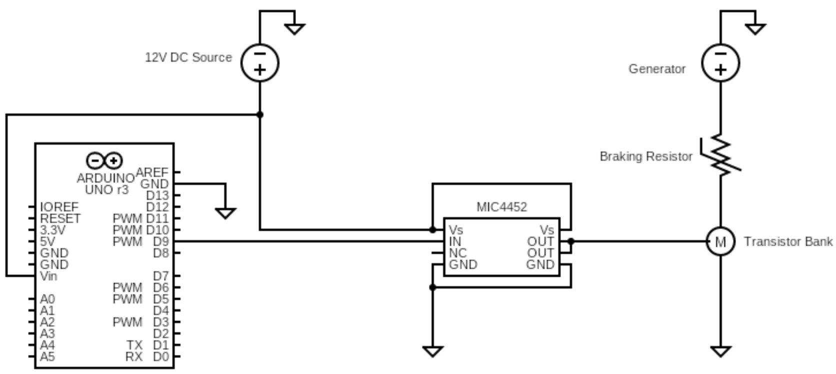

Figure 3.14: *The final iteration of the system schematic.*

3.3 Software Implementation

The software for this application was completely written for the Arduino integrated development environment (IDE). It is based on the C and the C++ languages, supplemented by other functions created to interact with the pins or the internal chips of the microcontroller. Any program based on this IDE has two fundamental functions: a setup() function, which is run only once and is usually used to initialize variables or impose pin modes, and a main() function, which executes cyclically with the GNU toolchain.

The Arduino IDE then converts the code into an encoded file which is loaded onto the Arduino board.

3.3.1 Arduino Programming

Several different programs were written for testing the system at various points of the development. The first iteration of the program consisted of a simple program where the analog variable imposed for the duty cycle would range from 0 to 255, effectively testing each and every possible value of the PWM signal. It would then loop back, decreasing to zero only to then rise back up, and so on. This program was mainly used for testing with the led diode, making it easy to see it working since the LED would fade up and down in brightness.

A second program was written where the value of the duty cycle imposed on the pulse-width modulated signal could be changed through the command line of the serial monitor. An image of the complete program can be found in the following code extract.

```
int pwmPin = 9;
int pwmNew = 0;
int pwmValue = 0;

void setup() {
  Serial.begin(9600);
}

void loop() {
  if (Serial.available() > 0) {
    int pwmNewPercent = Serial.parseInt();
    pwmNew = map(pwmNewPercent, 1, 100, 1, 255);
    if (pwmNew > 255) {
      Serial.println("ERROR! Insert a value between 1% and 100%");
    } else if (pwmNew > 0 && pwmNew <= 255) {
      Serial.print("I received: ");
      Serial.print(pwmNewPercent);
      Serial.println(" %");
      if (pwmNew > pwmValue) {
        Serial.println("Rising...");
        while (pwmNew > pwmValue) {
          Serial.print(pwmValue); Serial.print(" ");
          analogWrite(pwmPin, pwmValue);
          pwmValue += 5;
          delay(50);
        }
        Serial.println();
        Serial.print("PWM value reached: ");
        Serial.print(pwmNewPercent);
        Serial.println(" %");
      } else if (pwmNew < pwmValue) {
        Serial.println("Lowering...");
        while (pwmNew < pwmValue) {
          Serial.print(pwmValue); Serial.print(" ");
          analogWrite(pwmPin, pwmValue);
          pwmValue -= 5;
          delay(50);
        }
        Serial.println();
        Serial.print("PWM value reached: ");
        Serial.print(pwmNewPercent);
        Serial.println(" %");
      }
    } else {
      Serial.print("WRONG SERIAL: "); Serial.println(pwmNewPercent);
      Serial.print(" "); Serial.println(pwmNew);
    }
  }
  delay(500);
  float elapsedTime = millis();
  Serial.print("Looping OK, time: "); Serial.println(elapsedTime /
      1000);
}
```

In line 1, the pin 9 is assigned to the PWM signal output. In the successive lines some variables are initialized.
In line 6 the serial connection with the arduino is started at a rate of 9600 bits per second.
In line 11, the user is requested a percentage to set the duty cycle at. This value is then mapped to the 1-255 range in the successive line.
If the input value is plausible, that is positive and within 100%, the program will loop modulating the value set on the PWM pin in increments or decrements of 5, up until the requested mapped value, at which point the new duty cycle value will be printed on serial output.
This behavior is shown in lines 15 to 42.

The program will continuously loop, checking for serial input and printing a check up line every time it does so.

Through this code it is possible to select precise duty cycles for the output pulse-width modulated signal, while receiving confirmation of the correct outcome of the operation.

3.3.2 PID Software Implementation

The implementation of a PID control strategy was only conducted software wise. The hypothesized model required the addition of a torsiometer on the flexible joint inbetween the motor and the generator. This sensor would in fact allow for the system the complete the loop, enabling the control on the characteristics according to the input error.

A further possible implementation of the required hardware for the complete control loop would involve a sensor capable of registering the voltage and the current placed inbetween the transistor bank and the resistor element. Given these values, the braking torque could be easily derived through the formula

$$\tau = \frac{I \cdot V \cdot E \cdot 60}{RPM \cdot 2\pi}$$

where τ is the resulting braking torque, I is the current going through the resistor, V is the tension over the resistor, E is the efficiency (assumed to be around 85%), and RPM is the rotary speed read from the motor test bench.

A diagram of these possible solutions is shown in figure 3.15.

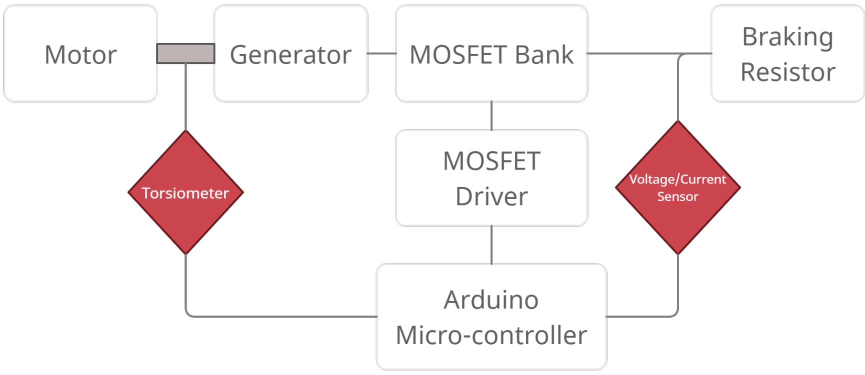

Figure 3.15: *Diagram of the possible PID control solutions.*

Such a system would make use of the computed torque to make corrections to its characteristics, in order to achieve a PID control.

The software that would allow this implementation has been again written for the Arduino IDE using the open source Arduino PID Library.
This control method involves firstly the tuning of the three tuning parameters K_p, K_d, K_i, which by consequence controls how the output is adjusted.
Furthermore, it makes use of an input variable, an output variable, and a Setpoint. Respectively, in our scenario, they represent the measured braking torque, the duty cycle percentage, and the effective braking torque we want to achieve. The program's main function is to read the measured torque, compare it to the setpoint, and modify the parameters of the software in such a way that the measured value is as close as possible to the setpoint. In our application the most impactful modifiable parameter is the duty cycle percentage, since it affects directly the braking torque.

The tuning of the three gain parameters can only be carried out with a complete system, but once it's completed the PID control software will automatically manage the characteristics of the system in order to keep the output steady and as close to the requested value as possible. The simple code written for the PID control implemented on Arduino is shown below, followed by its line-by-line explanation.

```
1	#include <PID_v1.h>
2	#define MeasuredTorque 5
3	#define PwmControlPin 6
4
5	double Setpoint, Input, Output;
6	double Kp=1, Ki=1, Kd=1;
7
8	PID myPID(&Input, &Output, &Setpoint, Kp, Ki, Kd, DIRECT);
9
10	void setup()
11	{
12	  Input = analogRead(MeasuredTorque);
13	  Setpoint = 1;
14	  myPID.SetMode(AUTOMATIC);
15	}
16
17	void loop()
18	{
19	  Input = analogRead(MeasuredTorque);
20	  if(myPID.Compute())
21	    analogWrite(PwmControlPin, Output);
22	  delay(50);
23	}
```

In the first three lines the library is included and the input (*MeasuredTorque*) and output (*PwmControlPin*) pins are defined.

In lines 5 and 6 the variables necessary for the control are defined. The three gains are here left at one.

In line 8, the function PID instantiates a new PID object defining input, output, setpoint, variables, and output direction.

In the setup function the *Setpoint* and *Input* are initialized, after which the PID object's mode is set to automatic control.

Finally in the loop function the input is continuously read every 50 milliseconds, and if the *Compute()* function returns true, the computed and modified *Output* value of the pulse-width modulated signal's duty cycle is written out. The *Compute()* function contains the PID algorithm, calculating a new Output value at a specific frequency which can be modified through the software function *SetSampleTime*.

The Compute() function makes the actual calculations that allow the PID control to take place, balancing the output from the measured input. Its code is shown below, followed by a summary explanation.

```
bool PID::Compute()
{
  if(!inAuto) return false;
  unsigned long now = millis();
  unsigned long timeChange = (now - lastTime);
  if(timeChange>=SampleTime)
  {
    double input = *myInput;
    double error = *mySetpoint - input;
    double dInput = (input - lastInput);
    outputSum+= (ki * error);

    if(!pOnE) outputSum-= kp * dInput;
    if(outputSum > outMax) outputSum= outMax;
    else if(outputSum < outMin) outputSum= outMin;

    double output;
    if(pOnE) output = kp * error;
    else output = 0;

    output += outputSum - kd * dInput;

    if(output > outMax) output = outMax;
    else if(output < outMin) output = outMin;
    *myOutput = output;

    lastInput = input;
    lastTime = now;
    return true;
  }
  else return false;
}
```

The function first makes a check on the time passed, in order to make the computations only with a certain specific frequency (*SampleTime*). It then computes all the working error variables.

It then checks if the proportional gain on measurement K_p and the proportional gain on error K_i variables are specified, in which case it adds their influence to the output.

Finally it computes the derivative gain's impact (K_d) on the *Output* variable, making the final modification for the control. It then saves a few variables for its next iteration.

Chapter 4

Data Analysis

In this chapter, the analysis that was carried out on the final system will be examined thoroughly, together with the results obtained. The final testing procedure was conducted first with the speed and torque controlled motor, tunable with the test bench, and afterwards with a three-phase motor capable of a constant speed of 98 RPM and a constant torque output of 10 Nm.

The measurements were taken with two different oscilloscopes set to different modes, one for voltage and one for current, used concurrently. The oscilloscopes were attached to the resistor's terminals, thus effectively measuring the dissipated power.

A schematic of the connections is shown in figure 4.1.

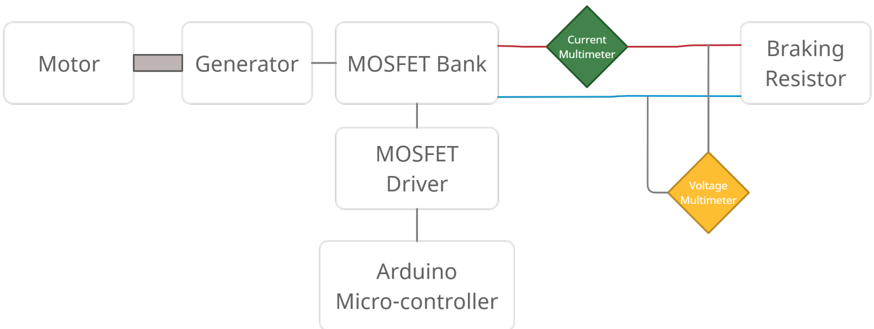

Figure 4.1: *Diagram showing the multimeter connections.*

As the test bench motor was only available for a restricted period of time, three tests were conducted at different engine velocities. A further test was carried out with the fixed speed motor. As a result, the readings for five different rotatory speeds were available: 98, 150, 200, 250 RPM.

In the following images, the graphs representing the current, voltage, electrical power, and torque as functions of the duty cycle are shown. Four different velocities were taken into consideration.

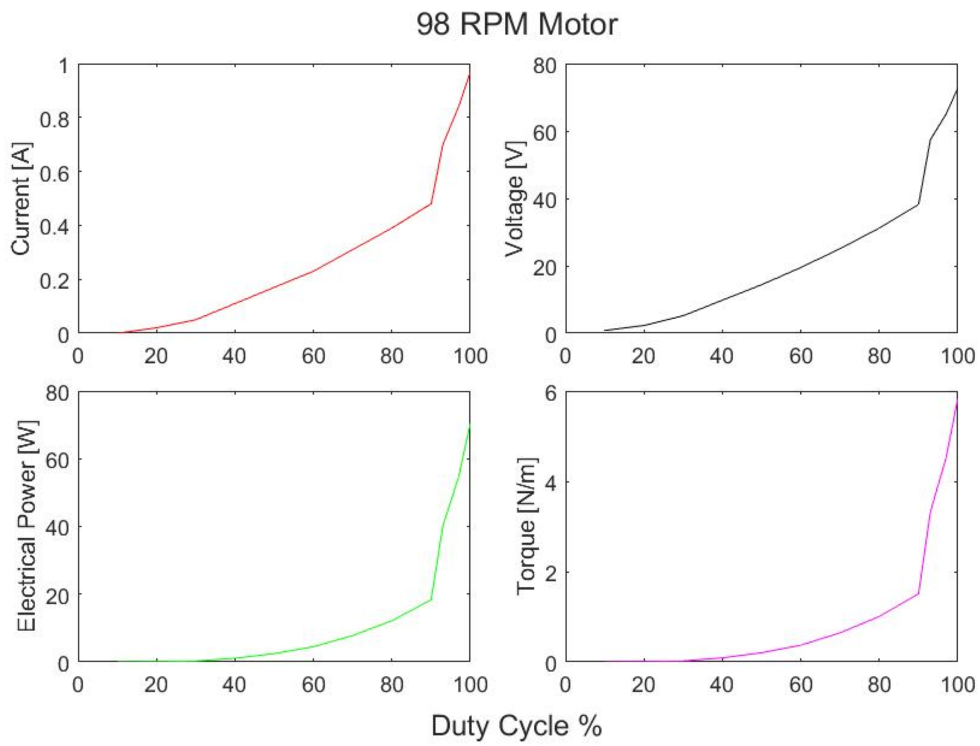

Figure 4.2: *From the upper left one, graphs representing current, voltage, power, and torque versus duty cycle percentage, at 98 RPM.*

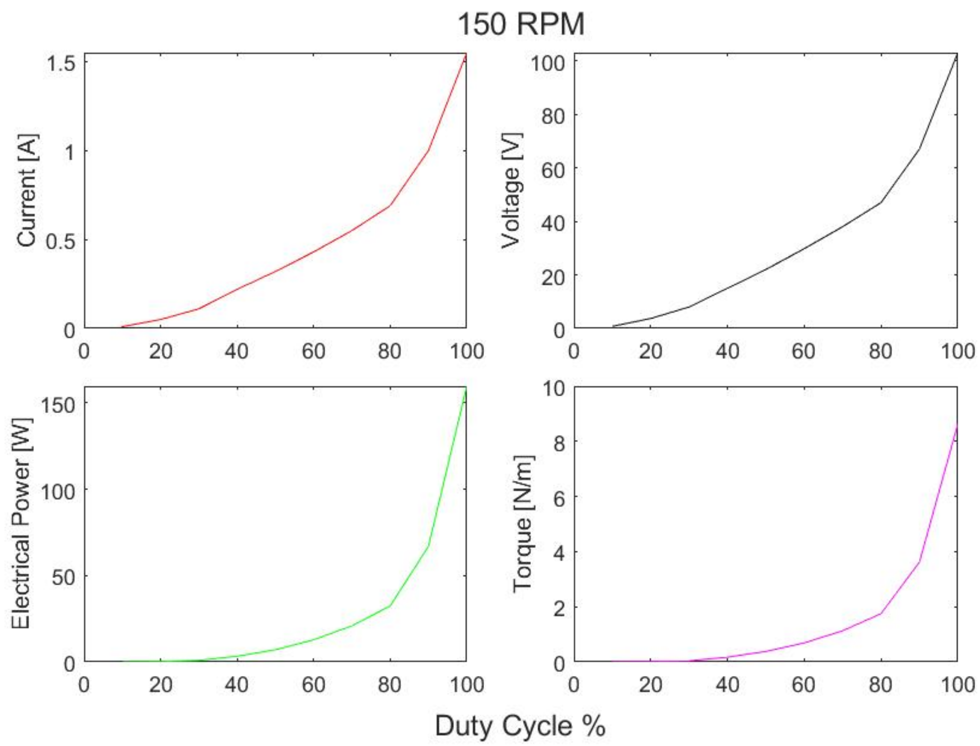

Figure 4.3: *From the upper left one, graphs representing current, voltage, power, and torque versus duty cycle percentage, at 150 RPM.*

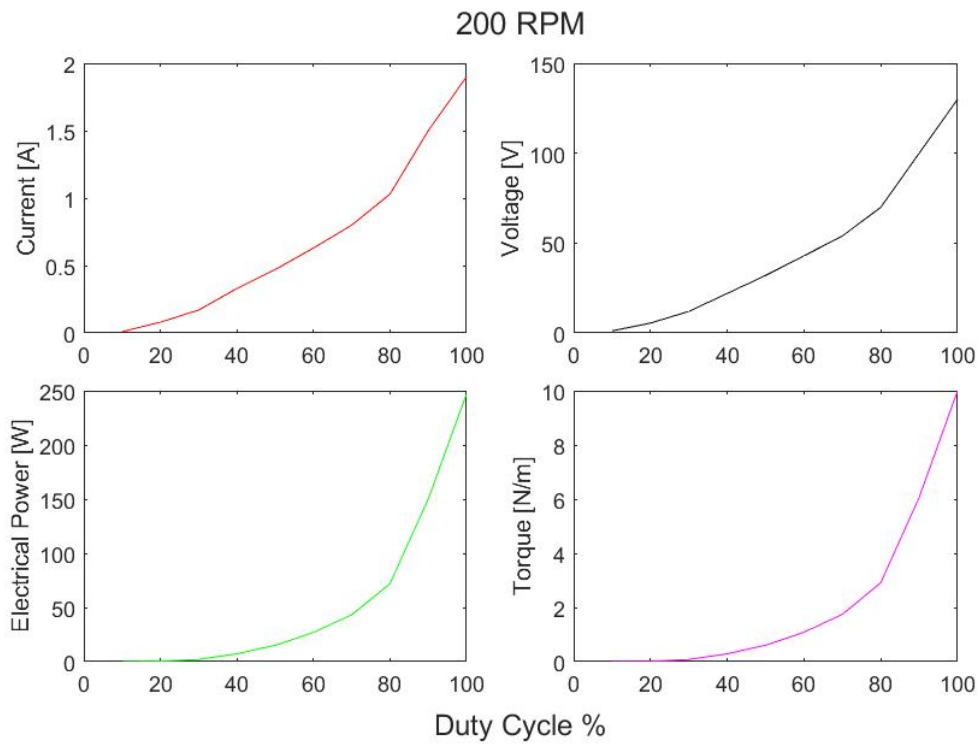

Figure 4.4: *From the upper left one, graphs representing current, voltage, power, and torque versus duty cycle percentage, at 200 RPM.*

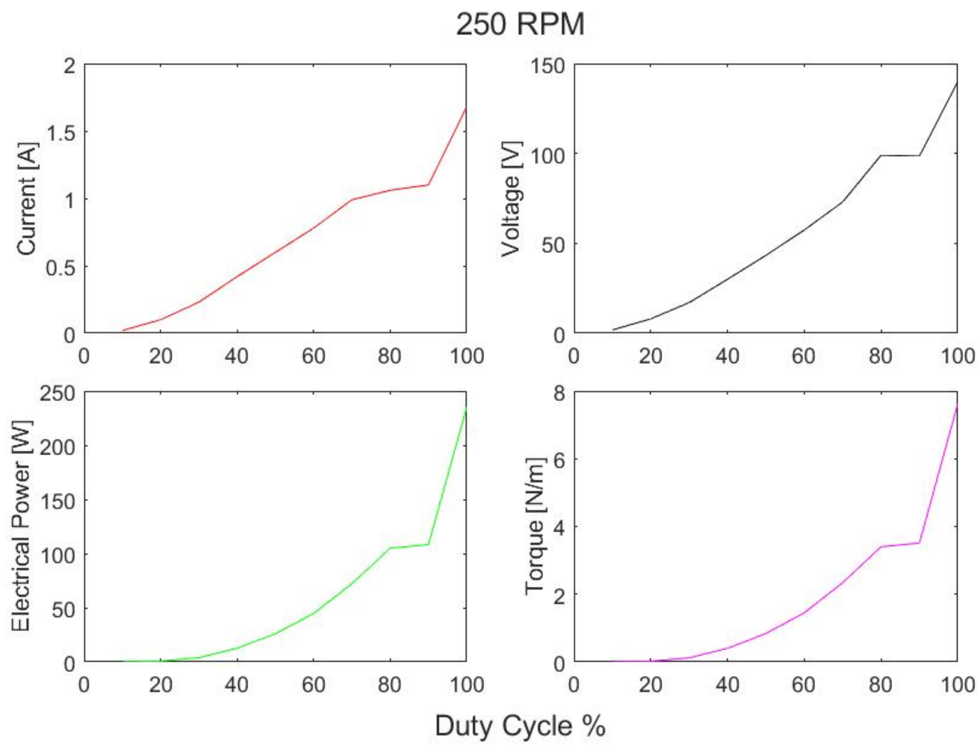

Figure 4.5: *From the upper left one, graphs representing current, voltage, power, and torque versus duty cycle percentage, at 250 RPM.*

From these graphs the behavior of the system can be deduced. An exponential relationship between the increase of the duty cycle percentage and the system's characteristics is clearly visible. The torque was derived from the formula $\tau = \frac{I \cdot V \cdot E \cdot 60}{RPM \cdot 2\pi}$ while the electrical power was derived from the formula $P = I \cdot V$.

An exponential increase of the parameters with the increase of the duty cycle and the speed is clearly noticeable. This behavior is expected given the nature of the dynamic braking system, and the employment of a generator as translator of mechanical power to electrical one. As such, the output electrical power will be higher as the speed of the motor becomes faster.

Furthermore, as the duty cycle percentage increases, so does the electrical power generated, and henceforth the braking torque offered by the system. In the conducted testing, a maximum value of 10 Nm of braking torque was measured, at the conditions of 100% duty cycle and 200 RPM of motor speed.
The characteristic of the system, represented by both a power over speed and a torque over speed graph, can be found in figure 4.6.

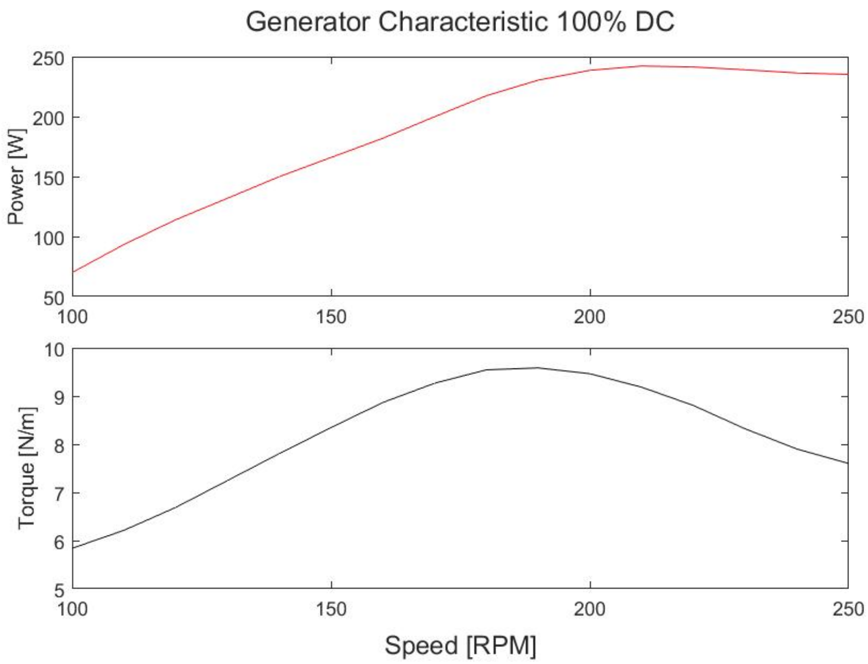

Figure 4.6: *Characteristic of the final system.*

From this final graph the behavior of the interfacing motor and generator can be clearly understood. It appears that the maximum power and therefore torque achievable is found at 200 RPM of rotatory speed. At higher velocities, the generated current diminishes, thus decreasing the torque generated. This is also influenced by the inability of the motor to supply enough torque to run consistently at 250 RPM. In fact, at 100% duty cycle the motor could not keep up a consistent 250 RPM, decreasing to 200 RPM.

From the characteristic of the system the maximum braking torque achieved is discovered to be at $T_{MAX} = 10.02Nm$. This value was found at in the 200 RPM scenario, with a duty cycle of 100%.

On the other hand, the maximum power measured at the braking resistor's terminals was found to be $P_{MAX} = 247W$, again in the 200 RPM and 100% situation.

Chapter 5

Conclusions

The system that was developed entailed a testing apparatus which allowed for a precise control of the braking torque imposed on a machine. The usage of several discrete components makes the model very flexible to a number of different applications. The absence of a disk brake or any friction among the model's elements makes it reliable and relatively maintenance free, requiring only a ventilation system for cooling purposes.

The implementation of the control software through the open source Arduino IDE makes the application open and straightforward. Furthermore, given the low cost of the board in question, the construction of such a system is quite affordable and of simple understanding.

The usage of distinct power MOSFETs allows for quick component replacement in case of damage or malfunctioning, even more so thanks to the mounting on terminal blocks.

The PID control method implemented through software allows for automatic correction of the system, ensuring that the imposed braking torque is maintained without severe fluctuations even in the presence of external disturbances.

The most important achievement is however the proof of concept, granting a clear understanding of the feasibility of this method for dynamic braking.

While this method is surely feasible, there exist other dynamic braking techniques which may be more suited to some applications. A downside of the developed solution is the requirement of several power MOSFETs to efficiently dissipate the generated electrical power. Moreover, the high amount of transistors implies the need for a fairly large container. The involvement of a generator as source of the power to be dissipated does entail a better working efficiency at higher RPM with respect to lower velocities, since the faster the alternator is turned the more current will be generated and the stronger will be the braking effect due to the resistor. Finally, the dissipation of the generated power has the consequence of a lot of heat being dissipated, thus requiring a cooling system to prevent possible component damage when testing over long periods or at high duty cycles.

Bibliography

1. Vehicle Braking Technologies: Advanced Emergency Braking System, Air Brake (Road Vehicle), Anti-Lock Braking System, Ausco Lambert Disc Brake, Automat

2. Dynamometer: Theory and Application to Engine Testing, Jyotindra S. Killedar, 25/08/2012

3. Analysis on Permanent Magnet eddy currents, URL: https://www.researchgate.net/publication/334162568

4. Magtrol, Hysteresis Brakes and Clutches

5. Electric Machinery Fundamentals, Stephen J. Chapman

6. Principles of Transistor Circuits: Introduction to the Design of Amplifiers, Receivers, and Other Circuits, Stanley William Amos

7. Three-phase systems, URL: https://www.sciencedirect.com/topics/engineering/three-phase-system

8. Hysteresis Braking, URL: http://publicationslist.org/data/barys.shyrokau/ref-9/EB2012-MS-25-Paper.pdf

9. Research on Regenerative Braking Systems: A Review September 2020International Journal of Science and Research (IJSR)

10. A review of regenerative braking systems, Dr. S. J. Clegg, URL: https://eprints.whiterose.ac.uk/2118/1/ITS105_WP471_uploadable.pdf

11. Arduino PID library, URL: https://playground.arduino.cc/Code/PIDLibrary/

12. Kiam Heong Ang, G. Chong and Yun Li, "PID control system analysis, design, and technology," in IEEE Transactions on Control Systems Technology, vol. 13, no. 4

13. R. Singh, S. Umashankar, D. Vijaykumar and D. P. Kothari, "Dynamic braking of induction motor - Analysis of conventional methods and an efficient multistage braking model," 2013 International Conference on Energy Efficient Technologies for Sustainability

14. PWM signal on arduino, URL: https://www.arduino.cc/en/Tutorial/Foundations/PWM